ROLE OF PERIPLASMIC NITRATE REDUCTASE ON DIAUXIC LAG IN DENITRIFYING BACTERIA

By

KIRANMAI DURVASULA

A DISSERTATION PRESENTED TO THE GRADUATE SCHOOL
OF THE UNIVERSITY OF FLORIDA IN PARTIAL FULFILLMENT
OF THE REQUIREMENTS FOR THE DEGREE OF
DOCTOR OF PHILOSOPHY

UNIVERSITY OF FLORIDA

2008

To my mom, Usha Sree, and my dad, Somayajulu.

ACKNOWLEDGMENTS

I thank my advisor, Dr. Spyros Svoronos and my co-advisor, Dr. Ben Koopman, for their support and guidance throughout my research. I thank my committee members (Dr. Yiider Tseng and Dr. Nemat O. Keyhani) for their advice and help. I also thank Dr. Madeleine Rasche and Dr. Yiider Tseng for allowing the use of their laboratory facilities.

I would like to acknowledge the alumni of our research lab (Ryan Hamilton, Anna Casasús-Zambrana and Dong-Uk Lee) for the initial training they provided. I also thank my fellow research members of my group (Kyle Fischer, Adrian Vega, Eric Staunton and Shourie Kapadi) for their help and friendship. Special thanks go to Kaemwich Jantama for all his advice.

Finally, I thank my mom, dad, and my husband for all their love and support and for just being there for me.

TABLE OF CONTENTS

page

ACKNOWLEDGMENTS 4

LIST OF TABLES 8

LIST OF FIGURES 9

LIST OF ABBREVIATIONS 11

ABSTRACT 13

CHAPTER

1 INTRODUCTION 15

2 EFFECT OF PERIPLASMIC NITRATE REDUCTASE (NAP) ON DIAUXIC LAG OF PARACOCCUS PANTOTROPHUS 26

Introduction 26
Materials and Methods 27
Growth Experiments 27
Nitrate Reductase Assays 31
Construction of a Nap-Deficient Mutant 32
Bacterial Strains and Plasmids 32
Nucleotide Sequence Accession Number 32
Genetic Techniques 32
Primer Design and PCR Conditions 35
Construction of pKD100 37
Deletion of *napEDABC* 38
PCR Verification of the Mutant 39
Results and Discussion 41
Conclusions 47

2 USE OF FLUORESCENCE IN SITU HYBRIDIZATION AS A TECHNIQUE FOR IDENTIFYING NAP^+ DENITRIFYING BACTERIA 48

Introduction 48
Materials and Methods 49
Probe Design 49
Chemicals 52
Bacterial Culture 52
Bacterial Isolates 53
Bacterial Fixation 53
The FISH Protocol 54
Results and Discussion 55

3 DIAUXIC GROWTH MODEL BASED ON NAP AND NAR SYNTHESIS KINETICS FOR DENITRIFYING BACTERIA 60

Introduction....60
Model....61
Rate of Synthesis of Nar....62
Rate of Synthesis of Nap....62
Oxic Growth....63
Specific Rate of Nitrate Uptake....63
Anoxic Growth....63
Materials and Methods....65
Growth Experiments....65
Optimization....66
Results and Discussion....67

4 FUTURE WORK....71

Introduction of *nap* Gene in a Nap-Deficient *Pseudomonas denitrificans*....71
Construction of Nar Probe using FISH....72
Colony Hybridization....73
Effect of the Carbon Substrate Reduction State on the Length of the Diauxic Lag....73

APPENDIX

A GENE DELETION STRATEGY....75

Step 1: Culture *E coli* Containing Helper Plasmid....75
Materials....75
Procedure....75
Step 2: PCR Amplification Kanamycin Resistance Gene from pACYC177 using Primers with *EcoR*I/ *Sph*I Restriction Sites....75
Materials....75
Procedure....75
Step 3: Clone PCR Fragment in pRVS1....77
Materials....77
Procedure....77
Step 4: Transformation of Donor Plasmid into Donor *E. coli*....78
Materials....78
Procedure....78
Step 5: Triparental Mating....80
Materials....80
Procedure....80
Step 6: Confirmation of the Mutant....80

B DIFFERENTIAL EVOLUTION....83

Initialization....83
Mutation....84

Crossover/Recombination....84
Selection....85

C DIAUXIC GROWTH MODEL SOURCE CODE....86

LIST OF REFERENCES....106

BIOGRAPHICAL SKETCH....110

LIST OF TABLES

Table		page
1-1	Enzymes of denitrification	20
2-2	Bacterial strains and plasmids used in this work	34
2-3	Primers used in PCR.	36
2-4	Enzyme activities of the wild-type and mutant	46
3-1	Percent homology of *napA* and *napB* subunits in four micro-organisms	49
3-2	Bacteria with a highly similar sequence to at least one candidate probe	50
3-2	Continued.	51
3-3	Performance of candidate probes against the test set of 71 bacteria	52
3-4	Percent correct identification for *nap* containing bacteria	52
3-5	Enzyme activity data and diauxic lag lengths compared to probe results	58
4-1	Parameter values obtained after fitting.	70
A-1	PCR reaction ingredients	76
A-2	Double digest reaction set up	78
A-3	Ligation reaction	78

LIST OF FIGURES

Figure		page
1-1	Nitrogen cycle	15
1-2	Organization of denitrification enzymes in the cell	19
1-3	Fluorescence in situ hybridization technique	23
2-1	Flowsheet for constructing Nap-deficient mutant KD102	33
2-2	Amplification of kanamycin cassette from pACYC177	37
2-3	Plasmid pKD100 (*napE'-Kan-napC'* cloned into pRVS1) constructed in the present work	38
2- 4	Verification of the mutant	40
2-5	Growth curves of four different denitrifiers	43
2-6	Comparison of lag lengths	44
2-7	Comparison of growth between wild-type and mutant	45
3-1	*Paracoccus pantotrophus* viewed at 600x magnification under incandescent light	56
3-2	*Paracoccus pantotrophus* viewed at 600x magnification under UV light after being treated with fluorescent probe that targets *napA*	56
3-3	*Pseudomonas denitrificans* viewed at 600x magnification under incandescent light	57
3-4	*Pseudomonas denitrificans* viewed at 600x magnification under UV light after being treated with fluorescent probe	57
3-5	Bacteria isolated from the University of Florida Waste Water treatment plant viewed at 600x magnification under incandescent light	59
3-6	Bacteria isolated from the University of Florida Water Reclamation Facility viewed at 600x magnification under UV light after being treated with fluorescent probe that targets *napA*	59
4-1	Model fit to the fermentor growth data of *P. pantotrophus*	68
4-2	Model fit to the fermentor growth data of the mutant	69
A-1	The PCR temperature profile used	76
A-2	Gel picture: desired fragment size	77

A-3 Blue colonies of *E. coli* DH5α harboring plasmid pKD100 79

A-4 Triparental mating 81

LIST OF ABBREVIATIONS

$a_{N, Nar}$	Maxiumum specific Nar synthesis rate
$a_{N, Nap}$	Maximum specific Nap synthesis rate
b	Specific biomass decay rate
b_{NO}	Specific nitrate reductase decay rate
CR	Crossover factor
D	Dimensions, Number of parameters to be optimized
e_{nap}	Specific Nap activity
$e_{nap,av}$	Average Nap activity
$e_{nap,max}$	Maximum Nap activity
$e_{nap,measured}$	Measured Nap activity
$e_{nap,max}$	Maximum Nap activity
$e_{nap,predicted}$	Predicted Nar activity from the optimization
e_{nar}	Specific Nar activity
$e_{nar,av}$	Average Nar activity
$e_{nar,max}$	Maximum Nar activity
$e_{nar,measured}$	Measured Nar activity
$e_{nar,predicted}$	Predicted Nar activity from the optimization
F	Scaling factor
F (g)	Objective function
g	Vector of D×1 decision parameters
K_1	Equilibrium constant for repressor/ inducer binding
K_2	Constitutive enzyme expression level
K_{Noi}	Half saturation co-efficient for internal nitrate
K_{OH}	Half saturation co-efficient for oxygen for aerobic growth

K_{Oi}	Half saturation co-efficient for oxygen inhibition for nitrate uptake
$K_{s,an}$	Half saturation co-efficient for carbon source for anoxic growth
$K_{s,ox}$	Half saturation co-efficient for carbon source for aerobic growth
n	Noisy random vector
NP	Number in the population
r_{anox}	Specific biomass growth rate under anoxic conditions
r_{ox}	Specific biomass growth rate under aerobic conditions
$r_{en,nar}$	Specific Nar synthesis rate
$r_{en,nap}$	Specific Nap synthesis rate
rnd( )	Uniform random number generator
r_{sni}	Specific nitrate uptake rate
S_s	Organic substrate concentration
S_N	Nitrate concentration
s_{ni}	Internal nitrate concentration
S_O	Dissolved oxygen concentration
t	Trial vector
V_{sni}	Maximum specific nitrate uptake rate
X_B	Biomass concentration
$X_{B,av}$	Average biomass concentration
$X_{B,predicted}$	Calculated values of biomass from the optimization
$X_{B,measured}$	Measured values of biomass
$Y_{c,an}$	Yield under anoxic conditions
$Y_{c,ox}$	Yield under aerobic conditions
η	Ratio of maximum growth on Nap to maximum growth on Nar
$\nu_{N,an}$	Nitrate consumed per unit biomass growth

Abstract of Dissertation Presented to the Graduate School
of the University of Florida in Partial Fulfillment of the
Requirements for the Degree of Doctor of Philosophy

ROLE OF PERIPLASMIC NITRATE REDUCTASE ON DIAUXIC LAG IN DENITRIFYING BACTERIA

By

Kiranmai Durvasula

December 2008

Chair: Spyros A. Svoronos
Cochair: Ben Koopman
Major: Chemical Engineering

Biological processes are preferred means of removing nitrogen from wastewater. It is achieved through alternating oxic and anoxic conditions. The period of little or no growth observed when switching from oxygen as terminal electron acceptor to nitrate as terminal electron acceptor is called diauxic lag. Lag periods reduce overall rate of nitrogen removal hence must be reduced. All denitrifiers have membrane bound nitrate reductase (Nar). However, some gram negative bacteria also express periplasmic nitrate reductase (Nap). The present research was carried out to investigate the effect of Nap on diauxic lag.

Growth experiments were done with four denitrifiers, two of which had Nap and Nar (*Paracoccus pantotrophus* and *Alcaligenes eutrophus*) and two had only Nar (*Pseudomonas denitrificans* and *Pseudomonas fluorescens*) to determine diauxic lag. It was found that the diauxic lag was shorter for the bacteria which had Nap. To conclusively prove that Nap is responsible for shorter diauxic lag, the gene *napEDABC* that encodes for Nap was deleted from *P. pantotrophus*. Simultaneous growth experiments along with enzyme activity measurements were carried out for the wild strain and mutant of *P. pantotrophus* to study diauxic lag. It was

found that diauxic lag has increased significantly for the mutant strain as compared to the wild strain.

The presence of Nap is usually determined by conducting enzyme assay measurements which is tedious and time consuming. To facilitate easy identification of bacteria containing Nap, we conducted a FISH (Fluorescence In-Situ Hybridization) probe that binds to Nap. The probe successfully tested against two *nap*$^{+}$ bacteria (*P. pantotrophus* and *A. eutrophus*) and two *nap*$^{-}$ bacteria (*P. denitrificans* and *P. fluorescens*).

A model is presented in which the growth kinetics and nitrate uptake where linked to the synthesis of Nar and Nap. The model assumes the existence of a nitrate respiration operon and links the activity of Nar to the nitrate uptake rate into the cell. It also assumes that Nap contributes to growth during transition from aerobic to anoxic phase. This model successfully matched the experimental data for growth and captured the shorter lag displayed by wild-type *P. pantotrophus* which has both Nap and Nar.

CHAPTER 1
INTRODUCTION

Nitrogen removal is an important component of wastewater treatment plants. Excess nitrogen in wastewater leads to eutrophication of receiving water bodies, and can cause harmful effects on aquatic life due to oxygen depletion. It is also toxic in some forms (Ramalho, 1983) and has adverse health effects. Nitrogen is commonly removed by biological means because they are both efficient and cost effective (Grady et al., 1999). Biological nitrogen removal consists of the processes of nitrification, oxidation of ammonia to nitrate, and denitrification, reduction of nitrate to dinitrogen (Figure 1-1).

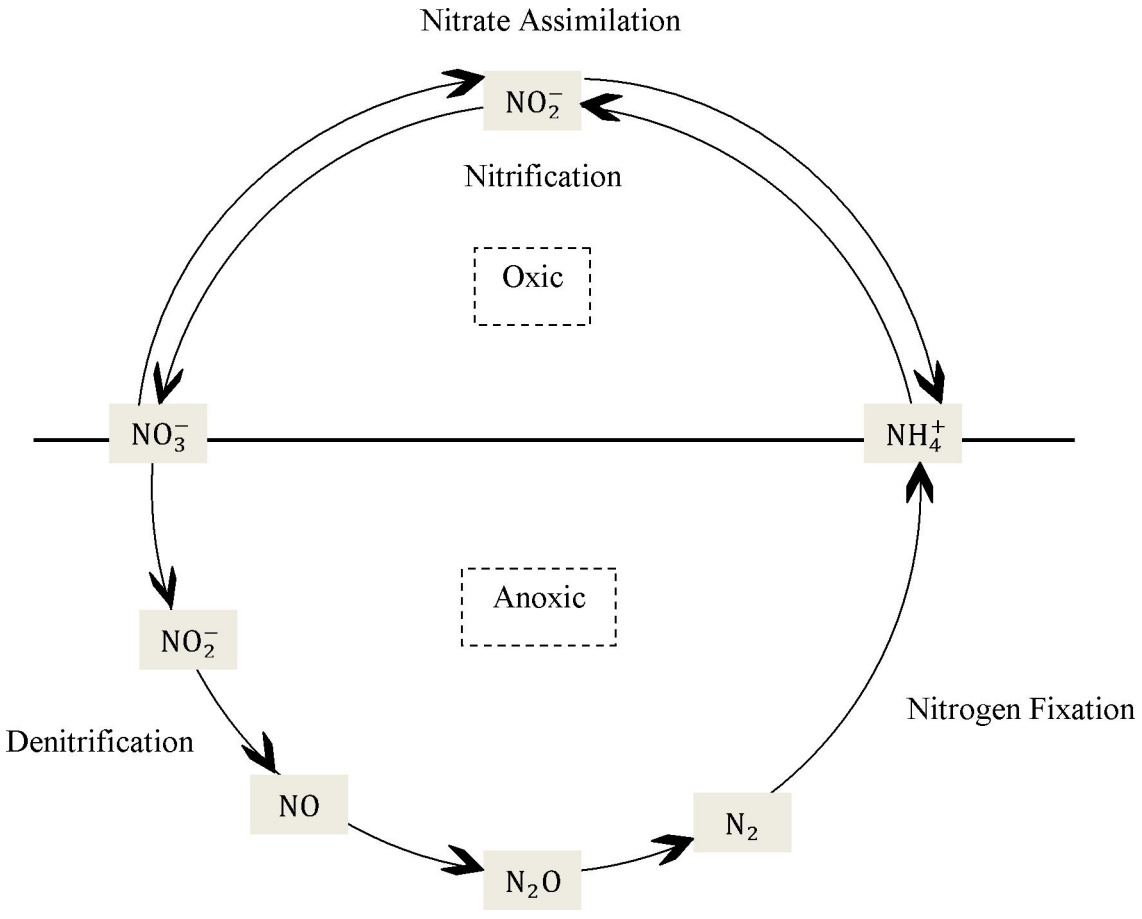

Figure 1-1. Nitrogen cycle

Although denitrification under aerobic conditions has been reported, the rate of denitrification is maximized under anoxic (dissolved oxygen absent, nitrate present) conditions (Tiedje, 1988). Therefore, to achieve nitrogen removal in a single-sludge system, a mixed population of nitrifying and denitrifying bacteria must be exposed to alternating aerobic and anoxic conditions (Ramalho, 1983). The biological nitrate reduction to dinitrogen is carried out by heterotrophic, facultative bacteria (*Paracoccus pantotrophus*, *Pseudomonas denitrificans*, *Pseudomonas fluorescens*, *Pseudomonas stutzeri*, *Alcaligenes eutrophus* etc). Denitrification has several intermediates such as NO_2^-, NO, N_2O. Many investigators (Waki et al., 1980; Liu et al., 1998a, 1998b; Gouw et al., 2001) have shown that when bacteria change from dissolved oxygen to nitrate as terminal electron acceptor, there may be a period of little or no growth. This period, when it occurs between two periods of exponential growth, was termed as diauxic lag by Monod (1942). The diauxic lag corresponds to the time necessary for bacteria to synthesize and activate the enzymes necessary to metabolize the less preferred substrate. Lag periods reduce overall rate of nitrogen removal, hence must be reduced.

The characteristic feature of gram negative bacteria is the presence of an extra outer membrane layer. The space between the outer membrane and the plasma membrane is the periplasmic space. The function of the outer membrane is to regulate the flow of the nutrients into the cell and waste products out of the cell. The outer membrane is basically a bilayer of lipids and contains channel forming proteins called porins. These porin proteins control the permeability of polar solutes across the outer membrane of gram-negative bacteria (Nikaido, 2003). There are at least two general pathways for the diffusion of small molecules across the outer membrane: one for hydrophobic and one for hydrophilic compounds. Porins create a water-filled pore through which ions and some small hydrophilic molecules can pass by

diffusion. The channels can be opened (or closed) according to the needs of the cell. The permeability of hydrophobic molecules depends on its partition co-efficient. Nitrate from the environment is transported into the periplasmic space through porins.

Different enzymes catalyze the different reduction reactions of denitrification (Table 1-1). Their location in the cell is mapped in Figure 1-2. Two types are dissimilatory nitrate reductases are found in bacteria: Membrane bound nitrate reductase (Nar) and Periplasmic nitrate reductase (Nap). All denitrifiers are believed to have membrane bound nitrate reductase (Nar). However, some gram negative bacteria also express periplasmic nitrate reductase (Nap) (Moreno-Vivián et al., 1999). Membrane bound nitrate reductase, which is anchored to the cytoplasm side of the membrane, allows ATP synthesis by using nitrate as the terminal electron acceptor under anoxic conditions. Nar gets the electrons from ubiquinol which generates proton motive force (PMF) and allows ATP synthesis. Ubiquinol is oxidized at the periplasmic side of the cytoplasmic membrane. These electrons are transported into the cytoplasm through the transmembrane protein and are utilized in the reduction of nitrate (Berks et. al., 1995).The Nar system is generally induced by nitrate and repressed by oxygen, but is insensitive to ammonium. Due to the cytoplasmic location of Nar, nitrate has to be transported into the cell before it can be reduced. Oxygen inhibits nitrate transport, thereby inhibiting nitrate reduction by Nar. The location of nitrite reductase makes it necessary for the nitrite produced inside the cell to be transported out to continue further reduction (Moreno-Vivián et al., 1999). The mechanism of nitrate uptake is not well understood. However, Wood et al. (2002) discuss the presence of two homologues of NarK transport protein – NarK1 and NarK2. They suggest that NarK1 is nitrate/proton symporter and NarK2 is a nitrate/nitrite antiporter. Nar is inhibited by azide (Bell et al., 1990) and chlorate in *Paracoccus pantotrophus* (Rusmana, 2004). The inhibition by azide

is achieved indirectly by controlling the movement of nitrate across the cytoplasmic membrane to the active site of its reductase (Bell et al., 1990). Chlorate inhibits Nar activity by blocking the nitrate transporters.

Periplasmic nitrate reductase which is on the periplasmic side of the membrane is not repressed by either nitrate or ammonium and maximally expressed under aerobic conditions (Moreno-Vivián et al., 1999). Chlorate and azide can be selectively used as inhibitors to distinguish between Nar and Nap activity in the bacteria.

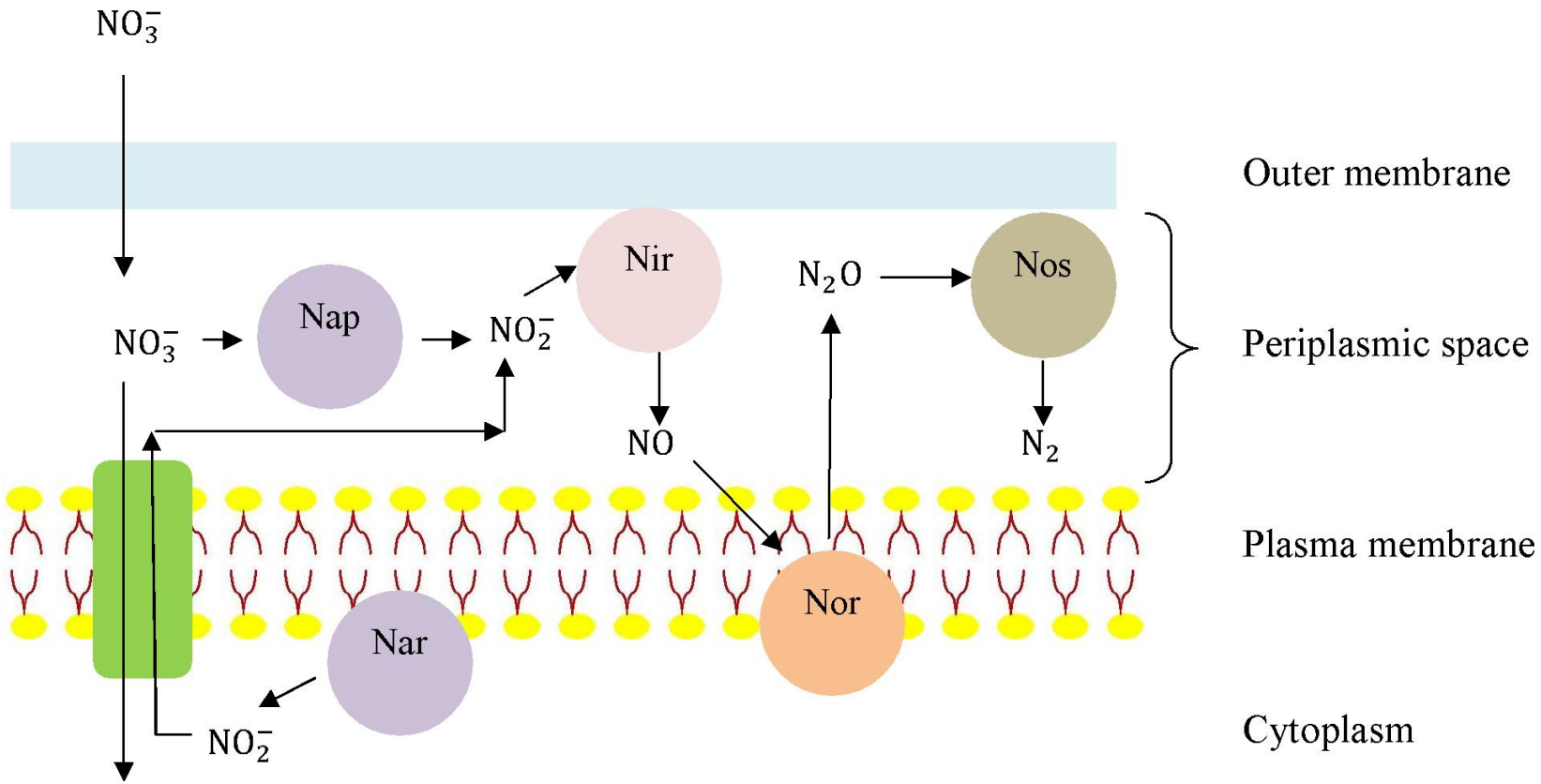

Figure 1-2. Organization of denitrification enzymes in the cell

Table 1-1. Enzymes of denitrification

Enzyme	Designation	Location	Reaction catalyzed
Nitrate reductase	Nar		$NO_3^- \rightarrow NO_2^-$
Membrane bound		Cytoplasm side of plasma membrane	
	Nap	Periplasm side of plasma membrane	$NO_3^- \rightarrow NO_2^-$
Periplasmic			
Nitrite reductase	Nir	Periplasmic space	$NO_2^- \rightarrow NO$
Nitric oxide reductase	Nor	Cytoplasmic membrane	$NO \rightarrow N_2O$
Nitrous oxide reductase	Nos	Periplasmic space	$N_2O \rightarrow N_2$

The function of periplasmic nitrate reductase is poorly understood. Proposed roles for periplasmic nitrate reductase are that it is used for redox balancing and adaptation to metabolism under anoxic conditions after transition from aerobic conditions (Moreno-Vivián et al., 1999). Several authors have suggested that Nap is used to shunt excess electrons to nitrate for redox balancing (Richardson and Ferguson, 1992; Sears et al., 2000). Redox balancing can be necessary for optimal bacterial growth under some physiological conditions, such as oxidative metabolism of highly reduced carbon substrates in aerobic heterotrophs (Moreno-Vivián et al., 1999). The level of Nap activity during aerobic growth has been shown to increase with the extent of reduction of the carbon substrate in cultures of *Paracoccus pantotrophus* (Sears et al., 2000). The transcription of *nap* operon is dependent on the reduction state of the carbon substrate used. The carbon substrate preference for growth is in the order succinate, acetate and butyrate. That is, the least preferred carbon substrate is the one which causes the greatest activation of *nap* operon (Ellington et al., 2002). With the increase in the reduction state of carbon, more electrons are available for transfer. This increases the yield of ATP and lower concentration of ADP in the

cell. Since phosphorylation of ADP is associated with the respiration, the lower concentration of ADP puts a constraint on the respiration rate of the cell (Ellington et al., 2002).

Diauxic lag has been studied by several researchers. The occurrence of lag when the terminal electron acceptor changes from oxygen to nitrate has been reported by Waki et al. in 1980. In 1998, Liu et al. found that the length of the diauxic lag in *P. denitrificans* is dependent on the length of the aerobic phase. Longer lags resulted from longer aerobic growth phases. They also found that the presence of nitrate during the aerobic phase has no effect on the length of the diauxic lag. The composition of the preculture had a significant effect on the diauxic growth. Here, preculture refers to the growth phase before the start of the diauxic growth experiment and the biomass from the preculture is used to initiate growth in the experiment. When bacteria were precultured under oxic conditions with nitrate absent, diauxic lags were longer than when bacteria were precultured in the presence of both oxygen and nitrate. Presence of nitrate during long aerobic phases somewhat compensated for the absence of nitrate during preculture phase. In experiments with anoxic preculture, short lags were usually observed when nitrate was absent from the aerobic phase. Even shorter lags or no lags at all, were observed when nitrate was present during the aerobic phase (Gouw et al., 2001).

Casasús et al (2007) tested a Nap deficient denitrifier (*P. denitrificans*) and a Nap containing denitrifier (*P. pantotrophus*) with different carbon substrates and observed that the Nap containing strain had either no lag or very short lag whereas the Nap deficient strain experienced lags of at least 5 hours. The possible explanation is that Nap is responsible for shorter lag and it aids in transition from aerobic to anoxic phase. If presence of Nap is the reason for shorter lags, it would be advantageous to promote the growth of Nap containing bacteria in a biological nitrogen removal processes as this would increase the overall efficiency.

In a wastewater treatment plant, we have bacterial populations employed in biological nutrient removal. Not all of the microorganisms in the population are complete denitrifiers; some are incomplete denitrifiers where nitrate doesn't fully get reduced to dinitrogen. One way to detect the presence of Nap in this population is to use a technique called Fluorescence in situ hybridization (FISH). FISH is a relatively new cytogenetic technique which can be used to detect the presence or absence of a specific DNA sequence. FISH requires a fluorescent probe which has sequences highly similar to the DNA sequence in question. Therefore, the efficacy of the FISH technique depends on a lot on the probe design. A probe has to be large enough to specifically bind to the target region but not large enough that it obstructs the hybridization process. The probe usually has a fluorescent molecule on one end (like fluorophore) which is bound to the quencher on the other end. In the native state, the probe doesn't fluoresce because of this binding. FISH is carried out on a microscopic slide (Figure 1-3). The sample cells are first fixed on the slide. Then they are denatured, a process that separates the complimentary strands within the DNA double helix structure, and a fluorescently labeled probe of interest is added to the denatured sample mixture. The probe hybridizes with the sample DNA at the target site as it reanneals back into a double helix. Once the probe hybridizes to the target, the fluorophore and the quencher come apart and the resulting fluorescence can be detected under UV light. This signal can then be observed through a fluorescent microscope. Presence of fluorescent signal indicates the presence of the gene targeted by the probe in the sample DNA (Wilderer et al., 2002).

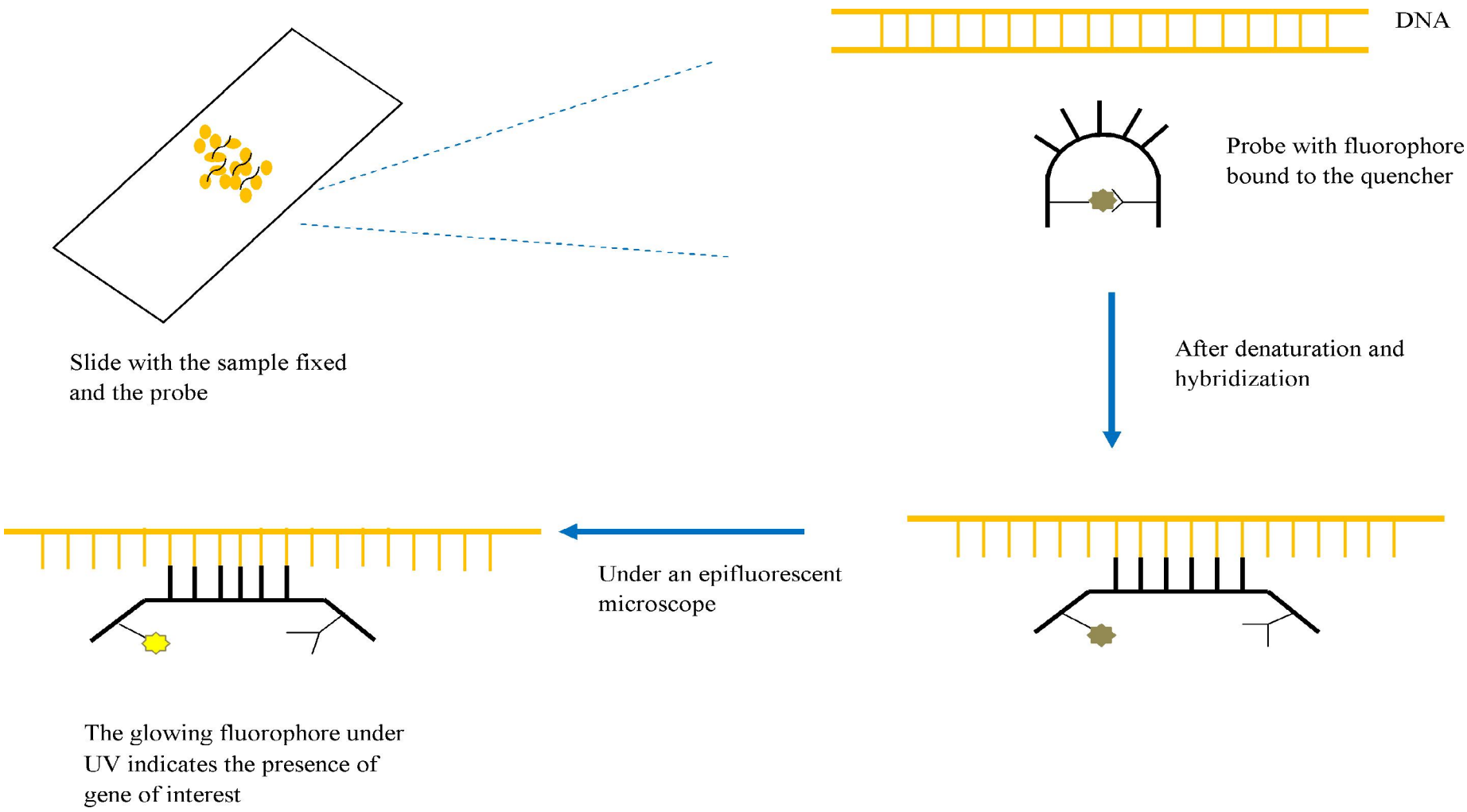

Figure 1-3. Fluorescence in situ hybridization technique

A great number of models have been proposed for biological denitrification. In most traditional models used in the industry, the role of diauxic lag has gone unrecognized on the overall kinetics of denitrification. Therefore the widely used Activated Sludge Models (ASM) 1, 2, 2d and 3 (Henze et al., 2000) do not portray the phenomenon of diauxic lag. Liu et al (1998a) used a cybernetic approach of Kompala et al (1986) where they modified ASM 1 to portray diauxic lag when the terminal electron acceptor switches from oxygen to nitrate. In this model they extended ASM-1 to incorporate nitrate reductase and oxygenase, the enzymes which catalyze growth under anoxic and aerobic conditions, respectively. In this model both enzyme concentration and relative activity affected growth rates, and a cybernetic term controlled enzyme synthesis. This model successfully predicted lag in activated sludge, but could not capture the much longer lags in pure cultures. This model was later modified to show the dependence of diauxic lag on the length of the aerobic phase and it was able to predict the typically longer lags obtained in case of *Pseudomonas denitrificans* (Liu et al., 1998b). A significant feature of this revised cybernetic approach was that the enzyme synthesis rate was an increasing function of enzyme concentration, implying that as enzyme was created, more cellular machinery and energy was available to facilitate further synthesis. A second alteration to the cybernetic approach was that a logistic function was used for the enzyme activity, instead of the term created by Kompala et al (1986). This modified model was able to portray the lag observed in pure cultures.

The model presented by Liu et al. (1998b) does not include the effect of substrate limitation when growth switches from anoxic to aerobic conditions. A further modification of this model was done to account for the enzyme specific level and the inhibitory effect of dissolved oxygen on nitrate reductase activity. This model also made sure that the metabolic

resources are not preferentially allocated to anoxic growth in the presence of oxygen (Casasús et al., 2001).

Hamilton et al (2005) considered the intracellular variables as well as the substrate concentrations in the solution. They discussed an approach which is based on the regulation of enzyme synthesis and active transport of nitrate into the cell of *P. denitrificans* which contains only the membrane bound nitrate reductase (Nar). They assumed the presence of nitrate respiration operon and that nitrate reductase and the nitrate transport protein are synthesized together and proportional to the amount of free operator. According to the model the rate of nitrate uptake into the cell is dependent on the concentration of nitrate reductase in the cell. The cellular nitrate levels induce the expression of Nar, which leads to anoxic growth and further uptake of nitrate from the environment. In this model, the diauxic lag was modeled solely on nitrate transport limitation. All the models discussed this far, have not taken into consideration the presence of periplasmic nitrate reductase (Nap) and the effect of Nap on diauxic lag.

CHAPTER 2
EFFECT OF PERIPLASMIC NITRATE REDUCTASE (NAP) ON DIAUXIC LAG OF PARACOCCUS PANTOTROPHUS

Introduction

Excess nitrogen leads to eutrophication of water bodies, disruption of aquatic life and is also toxic in some forms. Biological processes are preferred means of nitrate removal from wastewater because they are both efficient and cost effective (Grady et al., 1999). Biological nitrogen removal consists of the processes of nitrification (oxidation of ammonia to nitrate) and denitrification (reduction of nitrate to dinitrogen). This is typically achieved in wastewater treatment plants by operating biological reactors alternately under aerobic (nitrifying) and anoxic (denitrifying) conditions. When the bacteria switch from oxygen to nitrate as the terminal electron acceptor, there may be a period of little or no growth called the diauxic lag (Monod, 1942; Liu et al., 1998a, b; Gouw et al., 2001). Lag periods decrease the overall rate of nitrogen removal.

In denitrifying bacteria, there are two kinds of dissimilatory nitrate reductases – membrane bound nitrate reductase (Nar) located in the cytoplasm side of the plasma membrane and periplasmic nitrate reductase (Nap) located in the periplasm side of the plasma membrane. All denitrifiers have Nar, however some gram negative bacteria also express Nap. The *nap* operon is well characterized in some gram negative bacteria such as *P. pantotrophus* (Berks et al., 1995) and *A. eutrophus* (Siddiqui et al., 1993). *nap* operon is composed of different subunits in different organisms. The *napEDABC* operon of *P. pantotrophus* encodes for periplasmic membrane reductase with all its electron transfer components and proteins needed for the synthesis of fully functional enzyme. In *A. eutrophus,* it is *napAB* that encodes for periplasmic membrane reductase. Nap is predominantly expressed when cells are grown aerobically, but can operate in either the presence or absence of oxygen (Bell et al., 1990). The function of Nap in

denitrification is poorly understood. Suggested roles of Nap are that it is used for redox balancing (Richardson and Ferguson, 1992; Sears et al., 2000) and adaptation to metabolism under anoxic conditions after transition from aerobic conditions (Moreno-Vivián et al., 1999). In *Pseudomonas* sp. strain G-179, it was proposed that Nap catalyzes the first step in denitrification (Bedzyk et al., 1999). Casasús et al (2007) tested a Nap deficient denitrifier (*P. denitrificans*) and a Nap containing denitrifier (*P. pantotrophus*) with different carbon substrates and observed that the Nap containing strain had either no lag or very short lag whereas the Nap deficient strain experienced lags of at least 5 hours.

Based on the above information, we hypothesized that the presence of Nap in denitrifying bacteria substantially shortens or eliminates diauxic lag. In order to test this hypothesis, we formulated two objectives. The first objective was to screen Nap deficient and Nap positive pure cultures of denitrifying bacteria for the length of the diauxic lag. The second objective was to construct a Nap deficient mutant of a pure culture of denitrifying bacteria and then to characterize both the mutant and the wild-type for the length of diauxic lag.

Materials and Methods

Growth Experiments

Two Nap-deficient denitrifiers (*P. denitrificans, P. fluorescens*) and two Nap-positive denitrifiers (*A. eutrophus, P. pantotrophus*) were grown in minimal media as specified in Table 2-1. *P. denitrificans* was grown in a 1L fermentor (MultiGen model F-1000, New Brunswick Scientific, New Brunswick, NJ). The fermentor was stirred at 120 rpm and maintained at 37˚C. It was inoculated from an overnight culture to an absorbance of 0.1-0.11 at 550nm. The aeration was stopped and sparging of the reactor with nitrogen gas was initiated after at least one doubling of culture absorbance within the exponential phase under aerobic conditions. Two runs were performed. The other three species were grown in triplicate flasks containing 125mL of

minimal medium and were inoculated from an overnight culture to an initial absorbance of 0.1-0.15 at 550nm (*P. pantotrophus* and *P. fluorescens*) and at 436nm (*A. eutrophus*) (Siddiqui et al., 1993). The flasks were placed in a shaking incubator at 37˚C and 200 rpm. After at least one doubling of culture absorbance within the exponential phase under aerobic conditions, the flasks were removed from the shaker, sparged with nitrogen gas for 4 minutes, and then placed on a shaker within an anaerobic chamber (Coy Laboratory Type 'A', MI) held at 37˚C. Absorbance in all growth experiments was monitored using a Thermo-Spectronic Genesys 10UV spectrophotometer.

Further growth experiments with *P. pantotrophus* and Nap-deficient mutant (construction procedure described in the following section) of this species were carried out in triplicate 125 ml flasks as described above as well as in a 1L fermentor (Bio Flo 2000, New Brunswick Scientific New Brunswick, NJ). The growth experiment in the fermentor was stirred at 200 rpm and held at 37˚C. Aeration was provided at a rate of 3.0 L/min. The air was sterilized by passage through three 0.3 μm Whatman Hepa-Vent Glass microfiber filters in series and was humidified by bubbling through autoclaved deionized water. At the anoxic switch, nitrogen gas was substituted for the air. Since Casasús et al (2007) showed that the length of the diauxic lag was dependent on the carbon substrate used, a complex medium (Luria-Bertani) supplemented with 400mg NO_3^--N/L was used to avoid the possibility that an observed prolonged lag for the mutant was due to its inability to immediately utilize a particular carbon substrate under anoxic conditions. Two growth runs were carried out for the mutant in the fermentor. Kanamycin was added to a final concentration of 100 μg/mL in the growth medium for the triplicate flask runs and the first fermentor growth run. To ensure that kanamycin had no adverse effect on the growth, the second fermentor run was carried out with no kanamycin in the growth medium. Nitrate reductase

assays were carried out on biomass samples taken before the switch from aerobic to anoxic conditions and after the resumption of exponential growth in the anoxic phase. Lengths of diauxic lags exhibited during growth of the bacteria were calculated according to Lee et al (2008, in press).

Table 2-1. Minimal media recipe.

Chemicals	Concentration (g/L)			
	*P. pantotrophus**	*P. denitrificans***	*A. eutrophus**	*P. fluorescens***
Sodium acetate trihydrate	1.36	-	4.00	-
Glutamic acid	-	5.00	-	-
Malic Acid	-	-	-	4.00
Sodium phosphate dibasic	4.20	-	-	-
Potassium phosphate dibasic	-	5.00	5.00	5.00
Potassium phosphate monobasic	1.50	1.50	1.50	1.50
Sodium chloride	-	1.00	1.00	2.00
Ammonium chloride	0.30	1.00	0.30	1.00
Magnesium sulfate heptahydrate	0.10	0.20	0.10	0.20
Potassium nitrate	2.88	2.88	2.88	2.88
Trace metals	4 drops[a]	1 drop[b]	4 drops[a]	1 drop[b]

* - pH adjusted to 8.0-8.2, ** - pH adjusted to 7.0 – 7.2, a) Vishniac and Santer trace element solution (Vishniac and Santer, 1957), b) 0.5% of $CuSO_4$, $FeCl_3$, $MnCl_2$ and Na_2MoO_4. $2H_2O$.

Nitrate Reductase Assays

Nitrate reductase activity in intact cells was based on the rate of decolorization of reduced benzyl viologen (BV), which is proportional to the rate of electron transfer to nitrate (Jones et al., 1976). Centrifugation (11,300 RCF for 10 minutes at 4◦C) was used to harvest cells, followed by rinsing with 20 mM Tris buffer (pH 7). Cells were then suspended in 2 mL of the buffer. The reaction was carried inside an anaerobic chamber (Coy Laboratory Type 'A', MI) in two 4.5 mL disposable cuvettes of 1 cm optical path. To each cuvette was added the following: 2 mL of a solution of benzyl viologen and Tris buffer (0.3 mM BV, 20 mM Tris HCl), 200 µL of resuspended bacteria, 3 to 5 3-mm glass beads to facilitate mixing, and 25 µL of a 25 mM dithionite solution. A volume of 25 µL of 100 µM azide was added to one of the cuvettes as azide inhibits the activity of Nar. Additional benzyl viologen/Tris buffer was added to the cuvettes to completely fill the headspace and the cuvettes were then fitted with stoppers to maintain anaerobic conditions. The absorbance was monitored at 550 nm in a spectrophotometer (Thermo-Spectronic Genesys 10UV) programmed to take measurements every 15 seconds automatically. After 3 minutes, 35 µL of nitrate was injected into the cuvettes and the cuvettes were inverted twice before being returned to the spectrophotometer. At the end of seven minutes, air was allowed into the cuvette by removing the stopper for complete oxidation of benzyl viologen. The absorbance of biomass alone was measured. The total enzyme activity (Nap + Nar) is the difference between the negative slope of absorbance after addition of nitrate and before addition of nitrate in the cuvette with no azide added per unit absorbance. The analogous measurement from the cuvette with azide provides the Nap activity. Nar activity is obtained by subtracting Nap activity from total enzyme activity.

Construction of a Nap-Deficient Mutant

An outline of the procedure used for constructing the Nap-deficient mutant of *P. pantotrophus* is presented in Figure 2-1. The strategy was to construct a plasmid containing the gene for kanamycin resistance (kanamycin cassette) flanked by sequences homologous to the start and end of the *nap* operon, as well as *lacZ* as a selection marker. Introduction of this plasmid into the wild-type strain should result in the phenomenon of double crossover, in which the *napEDABC* gene is "deleted" through a replacement by the kanamycin resistance gene.

Bacterial Strains and Plasmids

All the bacterial strains and plasmids used in the experiments are as listed in Table 2-2.

Nucleotide Sequence Accession Number

The operon *napEDABC* encodes for periplasmic nitrate reductase in *P. pantotrophus* and can be can be retrieved from the NCBI website with the accession number Z36773.

Genetic Techniques

Standard techniques were used as described by Sambrook et al (1989) unless otherwise mentioned.

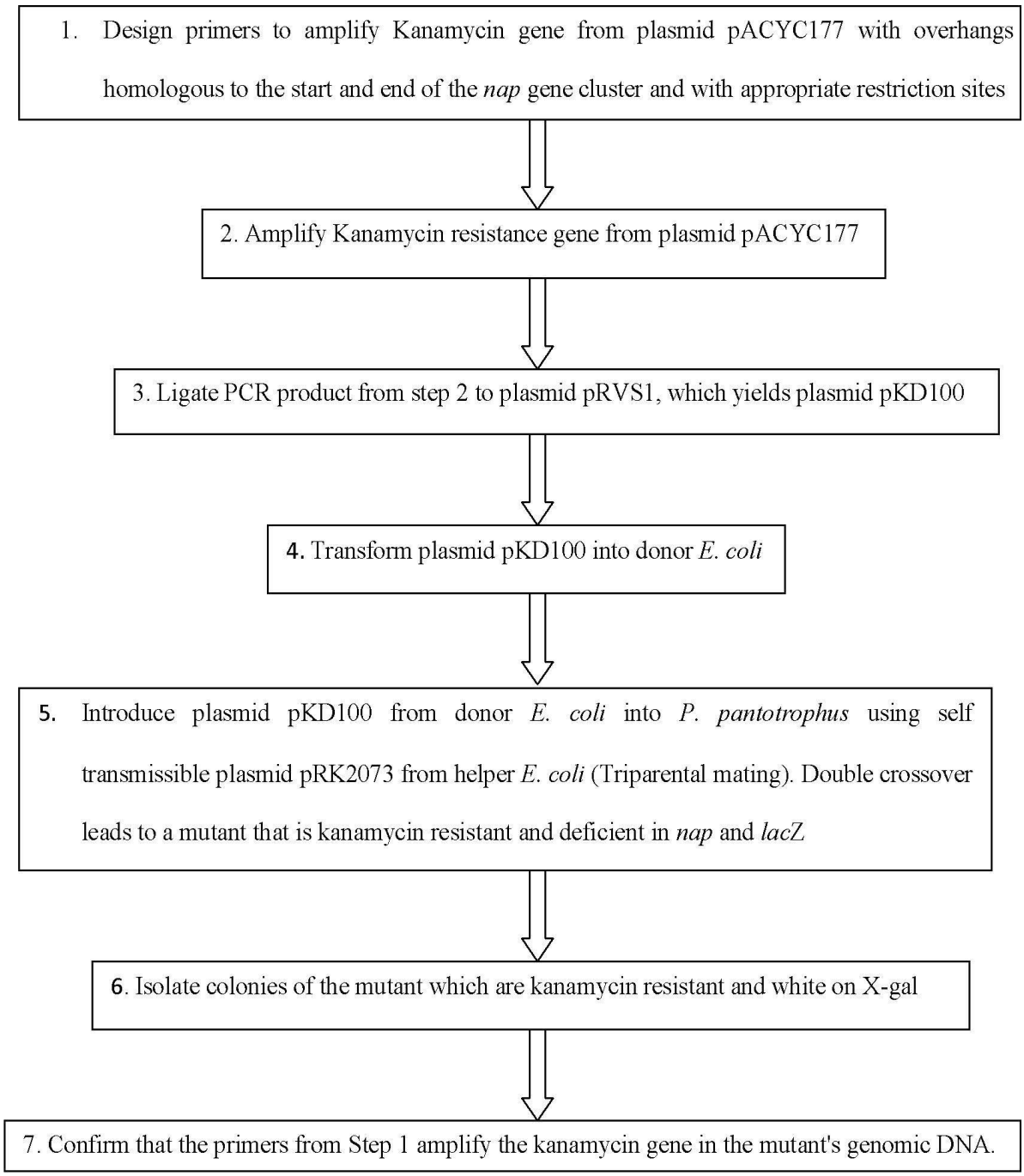

Figure 2-1. Flowsheet for constructing Nap-deficient mutant KD102

Table 2-2. Bacterial strains and plasmids used in this work.

Strain/ Plasmid	Relevant Characteristic(s)	Reference/ Source
P. pantotrophus strains		
GB 17	Wild-type	ATCC, VA
KD102	*napEDABC :: Kan*	Present Work
E. coli strains		
DH5α	*F⁻φ80dlacZΔM15 Δ(lacZYA-argF)U169 deoR, recA1 endA1 hsdR17(r_k^- m_k^+ phoA supE44 λ⁻ thi-1 gyrA96 relA1*	Zymo Research, CA
Plasmids		
pACYC177	Kan^r Amp^r	New England Biolabs, MA
pRVS1	Amp^r Sm^r, *oriV* (ColE1) *oriT* Tn*5p lacZ*	Van Spanning RJM et al., 1991
pRK2073	Mobilization helper plasmid (Tm^r)	ATCC, VA
pKD100	Amp^r Kan^r; *napE'-Kan-napC'* cloned into pRVS1	Present work

Primer Design and PCR Conditions

Kanamycin cassette from pACYC177 was amplified (Figure 2-2) using the primers listed in Table 2-3. The forward and the reverse primers included 20-nt sequences homologous to the plasmid regions upstream and downstream of the target gene (Kanamycin), appropriate restriction sites (*EcoR*I and *Sph*I) with required extra bases, and 40-nt overhangs homologous to the start and end of *napEDABC* (Datsenko et al., 2000). The reverse primer also included a set of stop codons in all six reading frames to ensure that the genes downstream of *napEDABC* were not affected by the ensuing deletion of this gene. PCR was carried out using the *Taq* polymerase (Qiagen, CA) and the product of length 1094 bps was verified using agarose gel electrophoresis. PCR product was then precipitated by the ethanol precipitation method.

Table 2-3. Primers used in PCR.

Description	Sequence 5' to 3'
Forward	AGACGGAATTC ATGATCGATTCCGCGAAAGAAACCGATCGTCCCAAGCACC R_f O_f ACAAAGCCACGTTGTGTCTC O_f K_f
Reverse	AGCAGCGCATGCA TTAATTAATT ACTAGCGCGTCTCGACGGTGGCGAGATAGCGGTGGACGGCC R_r S O_r CCGTCAAGTCAGCGTAATGC K_r

R) Restriction site with extra nucleotides. O) Overhang homologous to *nap*; K) Sequence to amplify kanamycin. S) Stop codons in all six reading frames. Subscripts: f) forward r) reverse.

Construction of pKD100

PCR product containing kanamycin gene and pRVS1 (Van Spanning et al., 1991) were digested in separate 500µL centrifuge tubes with *EcoR*I and *Sph*I restriction enzymes, respectively, for an hour at 37˚C. The digestates were combined, allowing ligation of *EcoR*I/*Sph*I restricted PCR product into *EcoR*I/*Sph*I restricted pRVS1 to generate a new plasmid (pKD100) (Figure 2-3) with sequences homologous to the start and end of *napEDABC* and with the gene for kanamycin resistance.

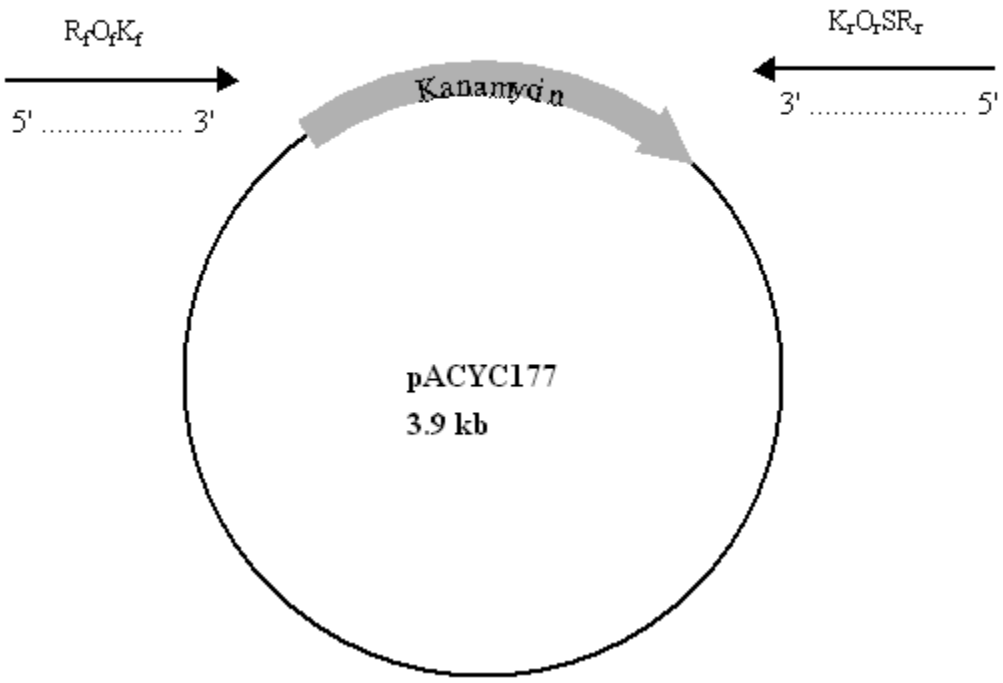

Figure 2-2. Amplification of kanamycin cassette from pACYC177. R) Restriction site with extra nucleotides. O) Overhang homologous to nap. K) Sequence to amplify kanamycin. S) Stop codons in all six reading frames. Subscripts: f) forward r) reverse.

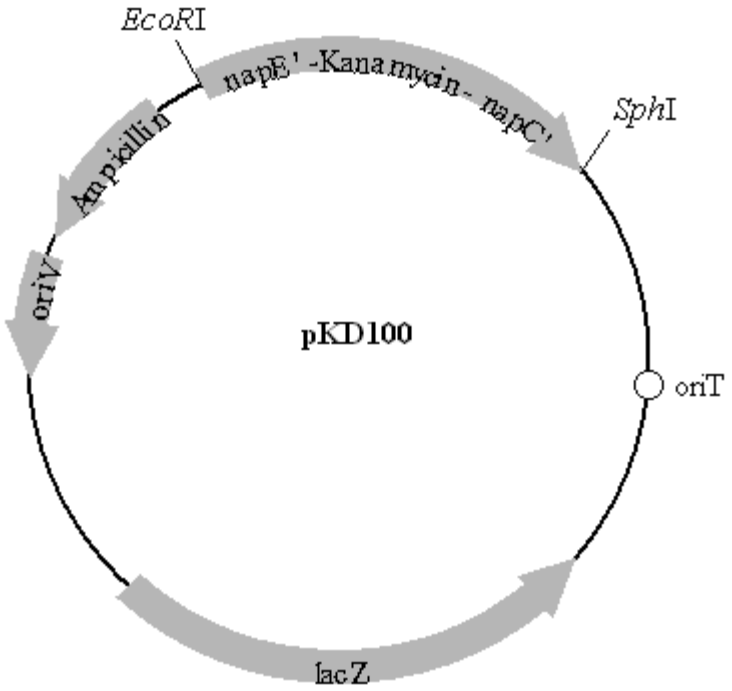

Figure 2-3. Plasmid pKD100 (*napE'-Kan-napC'* cloned into pRVS1) constructed in the present work

Deletion of *napEDABC*

The plasmid pKD100 was transformed into *E. coli* DH5α by heat shock at 42°C for 30 seconds, followed by cooling on ice for 5 minutes. The transformants were selected from LB agar plates supplemented with kanamycin (25μg/mL) and X-gal (40μg/mL). A triparental mating (Goldberg and Ohman, 1984) was carried out to introduce pKD100 into the wild-type *P. pantotrophus*. The plasmid pRK2073 in *E. coli* DF1020 served as the helper plasmid. *E. coli* DH5α/pKD100, *E. coli*/ pRK2073 and *P. pantotrophus* wild-type were added in a 1:1:3 ratio to 5mL Luria-Bertani (LB) solution. After 2 hours of growth, the mixture was filtered through a 0.45 μm filter (Gelman Sciences, MI) and was placed cell side up on LB agar plate. After incubating the plate for 24 hours, the filter paper with the bacteria on it was resuspended in 2 mL LB. Several 10-fold serial dilutions were performed in LB. A 100 μL aliquot of each dilution

was plated on LB agar supplemented with kanamycin (100 μg/mL) and X-gal (40 μg/mL) and the plates were incubated at 37˚C. The resulting ex-conjugants were white colonies, kanamycin resistant, and trimethoprim sensitive.

PCR Verification of the Mutant

The deletion of *napEDABC* in wild-type *P. pantotrophus* was verified by performing PCR controls. First, PCR was performed with the same primers used for amplification of the kanamycin cassette from pACYC177. The plasmid pKD100 was used as the positive control and wild-type *P. pantotrophus* as the negative control. Both the mutant and the plasmid pKD100 have a band at about 1000bps indicating the presence of the kanamycin cassette (1094 bps), whereas the wild-type *P. pantotrophus* does not exhibit a band in this region (Figure 2-4A). Then to ensure a correct double crossover, PCR was carried out with the wild type and the mutant using sequences upstream and downstream of *nap* as primers. As seen in Figure 2-4B, the wild-type has a faint band at approximately 4,300 bps, which corresponds to the *nap* operon (4,293 bps), whereas the mutant has no band at this position and a strong band at 1000 bps, which corresponds to the kanamycin cassette. Finally, one PCR was carried out with the wild-type and the mutant using a forward primer upstream of *nap* and reverse primer towards the end of kanamycin, and another PCR was carried out with the wild-type and the mutant using a forward primer at the start of kanamycin and reverse primer downstream of *nap*. In both cases, we see no amplification with the wild-type and a band at approximately 1000 bps which corresponds to the kanamycin cassette with the mutant (Figure 2-4C).

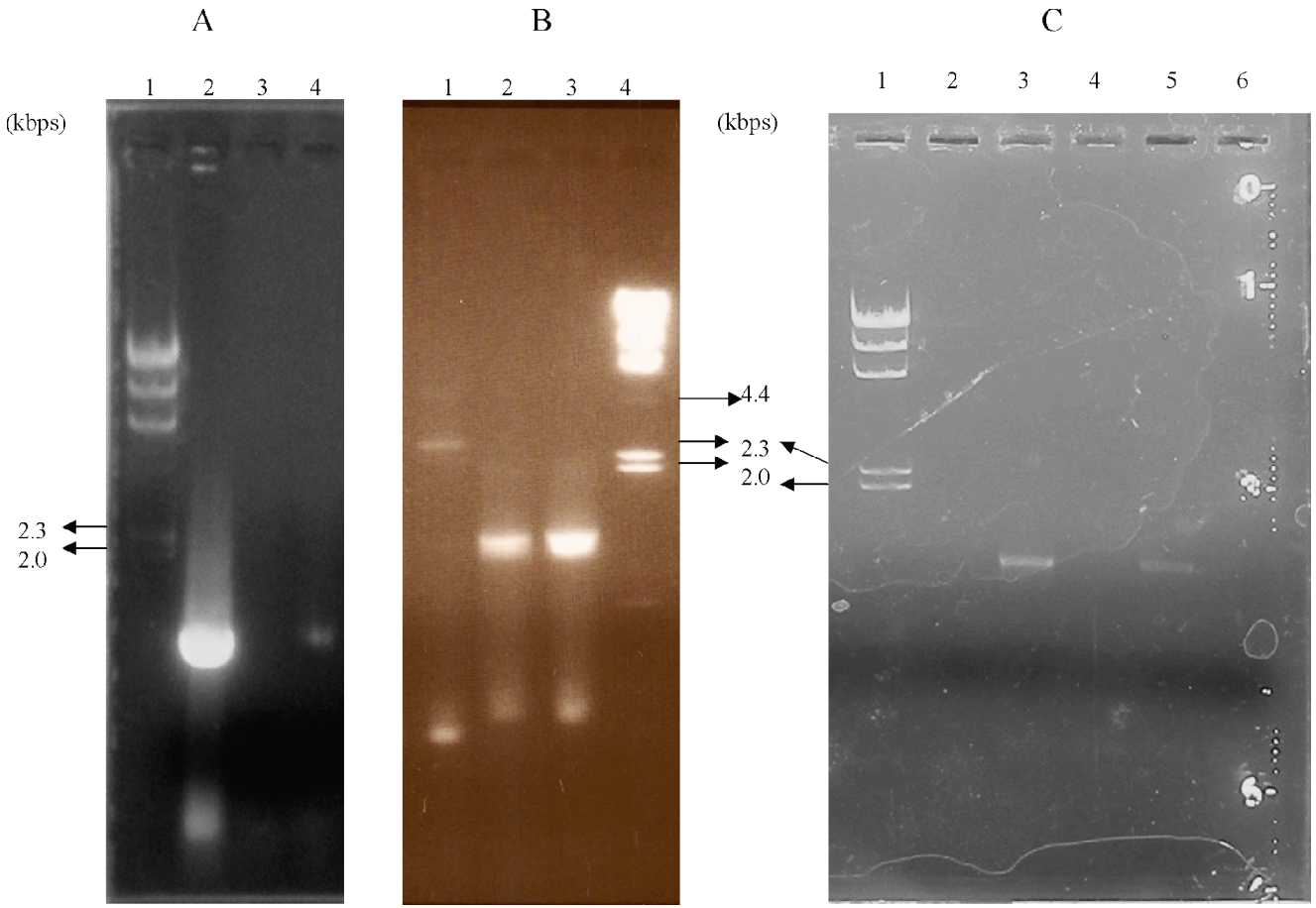

Figure 2- 4. Verification of the mutant. A) With same primers used for the amplification of kanamycin cassette from pACYC177 (Lane 1 - λ/*Hind* III marker, Lane 2 - pKD100, Lane 3 - *P. pantotrophus*, Lane 4 - Mutant), B) With primers upstream and downstream of *nap* (Lane 1 - *P. pantotrophus*, Lanes 2 and 3 - Mutant, Lane 4 - λ/*Hind* III marker, C) With forward primer upstream of *nap* and reverse primer towards the end of kanamycin (Lane 1 - λ/*Hind* III marker, Lane 2 - *P. pantotrophus*, Lane 3- Mutant) and forward primer at the start of kanamycin and reverse primer downstream of *nap* (Lane 3 - *P. pantotrophus*, Lane 4 - Mutant).

Results and Discussion

Growth curves for the four denitrifying bacteria (wild-types) are shown in Figure 2-5. The Nap-deficient bacteria *P. denitrificans* and *P. fluorescens* (Figures 2-5A and 2-5B) exhibited noticeably longer lags than the Nap-positive bacteria *A. eutrophus* and *P. pantotrophus* (Figures 2-5C and 2-5D). The lag lengths (Figure 2-6) were in the range of 9.6 to 11.1 hr for Nap-deficient bacteria, whereas the Nap-positive bacteria had lags ranging from 0 to 1.3 hr. One-way ANOVA indicated a significant effect of bacterial species on diauxic lag ($\alpha = 0.001$). Comparison of the lengths of the diauxic lags using Tukey's *post-hoc* test (Mendenhall and Sincich, 2007) at a significance level of 0.001 indicates that the lags of the Nap-positive bacteria (*P. pantotrophus* and *A. eutrophus*) are significantly shorter than those of the Nap-deficient bacteria (*P. denitrificans* and *P. fluorescens*).

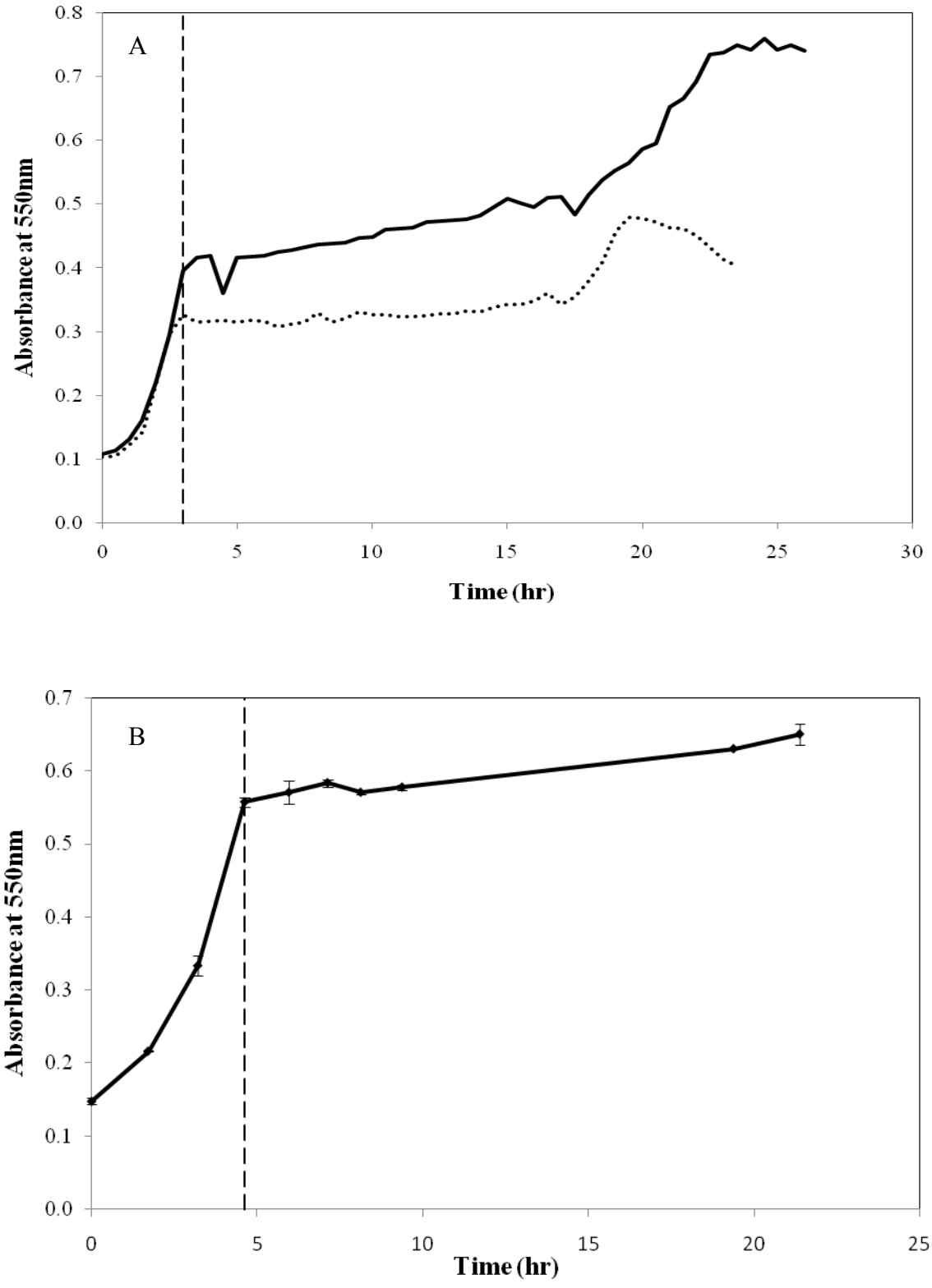

Figure 2-5. Continued.

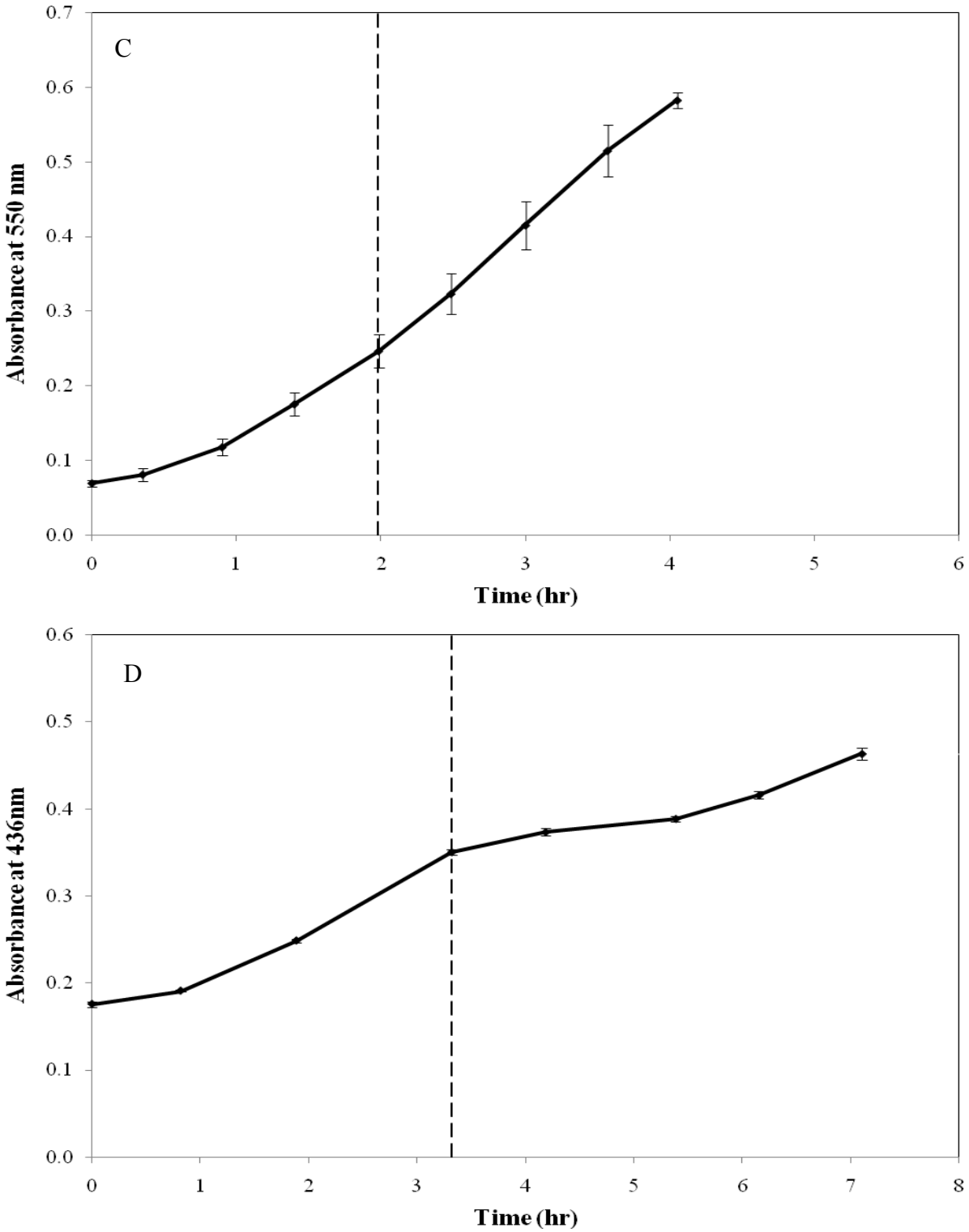

Figure 2-5. Growth curves of four different denitrifiers. A) *Pseudomonas denitrificans* , B) *Pseudomonas fluorescens*, C) *Alcaligenes eutrophus*, D) *Paracoccus pantotrophus.* The vertical dashed line indicates the switch to anoxic phase from aerobic phase. A) Two runs in the fermentor. B, C, D) Results of triplicate flasks with error bars denoting ±1.0 standard deviation.

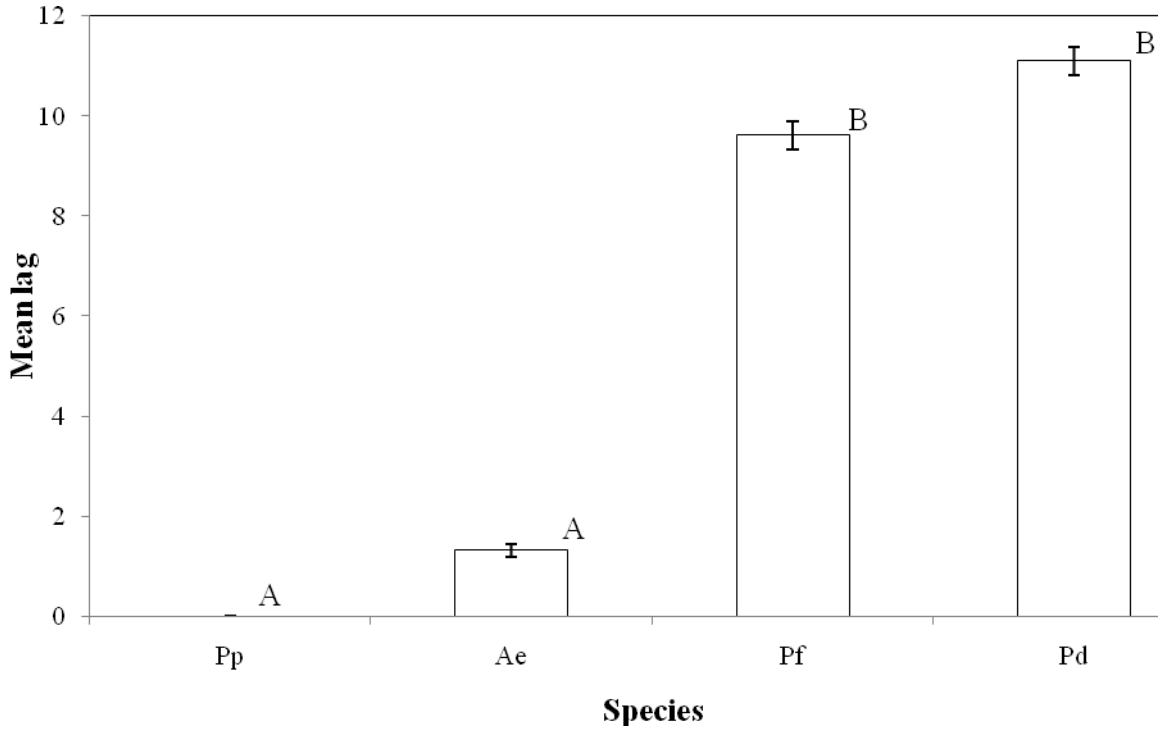

Figure 2-6. Comparison of lag lengths. Pp) *P. pantotrophus,* Ae) *A. eutrophus*, Pf) *P. fluorescens*, Pd) *P. denitrificans.* Means with same letter are not significantly different at $\alpha = 0.001$, as determined by Tukey's *post-hoc* test.

To further test the hypothesis that Nap shortens diauxic lag, we engineered a mutant of *P. pantotrophus* (named KD102) in which the *nap* operon was replaced by a kanamycin-resistance gene. A PCR of the mutant's genomic DNA with the same primers used to amplify the kanamycin gene from the plasmid, pACYC177, yielded the same band in the agarose gel electrophoresis as the plasmid, pKD100, indicating the presence of the kanamycin resistance gene, and hence a successful replacement of the *nap* operon in the mutant.

Figure 2-7A shows the result for one run in triplicate growth flasks for the wild-type and two runs in triplicate growth flasks for the mutant strain. The wild-type (Nap-positive) had short lags of 0.3 ± 0.1 hr. In contrast, the mutant (Nap-deficient) exhibited long lags (18.0 ± 1.0 hr and

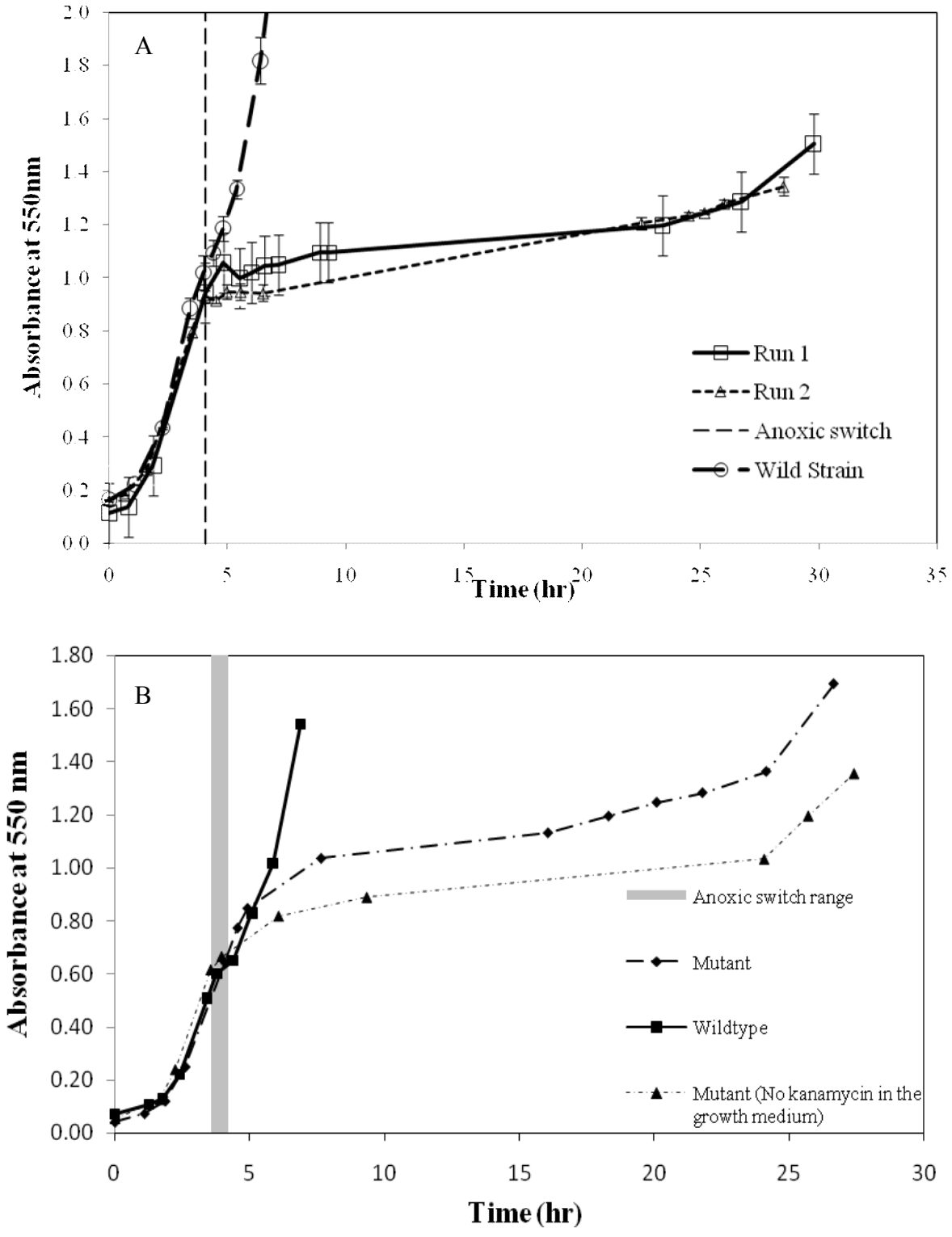

Figure 2-7. Comparison of growth between wild-type and mutant. A) Runs carried out in triplicate flasks, B) Runs carried out in fermentors.

12.4 ±1.3 hr). Measurements of enzyme activity (Nap and Nar) before the anoxic switch and after exponential growth under anoxic conditions was established were taken for the triplicate wild-type flask run and one of the two triplicate mutant flask runs. The results are shown in Table 2-4. As expected, the mutant shows no measurable Nap activity, while the wild-type did exhibit Nap activity. The flask runs showed Nar activity before the anoxic switch and higher activity after anoxic exponential growth was established. Pre-diauxie Nar levels were not equivalent, however, complicating interpretation of the results.

Table 2-4. Enzyme activities of the wild-type and mutant.

Run	Species	Before anoxic switch		During anoxic exponential phase	
		Nar	Nap	Nar	Nap
Flasks	Wild-type	2.91 ± 1.45	0.33 ± 0.17	5.02 ± 2.76	0.60 ± 0.12
	Mutant	0.41 ± 0.27	0.03 ± 0.06	0.83 ± 0.15	0.00 ± 0.00
Fermentor	Wild-type	0.03 ± 0.03	0.19 ± 0.06	1.54 ± 0.20	0.13 ± 0.11
	Mutant	0.04 ± 0.02	0.01 ± 0.01	0.39 ± 0.24	0.02 ± 0.02
	Mutant (No kanamycin in the growth medium)	0.04 ± 0.04	0.04 ± 0.06	0.89 ± 0.33	0.00 ± 0.00

Units: μmol BV^{+} oxidized $L^{-1}s^{-1}$per unit absorbance

The Nar activity exhibited at the end of the aerobic phase was attributed to insufficient aeration in the flask experiments. To suppress pre-diauxie Nar activity, we repeated the experiments in a fermentor, which allowed a higher aeration rate. Figure 2-7B depicts the results of the experiments in the fermentor. The wild-type (Nap-positive) had short lag of 0.4 hr while the mutant (Nap-deficient) exhibited a long lag of 11.5 hr (with kanamycin in the medium) and 9.3 hr (with no kanamycin in the medium). As can be seen from Table 2-4, Nar activity before the anoxic switch was near zero for both the mutant and the wild-type. As expected, Nar activity increased substantially when anoxic exponential anoxic growth was achieved. Nap was absent in the mutant and present in the wild-type. Given the nearly identical pre-diauxie Nar activities and

the difference in Nap activities, it can be concluded from the data that deletion of the *nap* operon (and thus elimination of Nap activity) was the cause of the significantly increased diauxic lag.

The information gained in this study opens the door to significant improvement in nitrogen removing wastewater treatment plants. Understanding the influences of design, plant operation, and wastewater characteristics on populations of Nap^+ bacteria can ultimately lead to strategies for enrichment of these denitrifiers. The resulting decrease of diauxic lag would lead to higher overall denitrification rates.

Conclusions

Up to now, the role of Nap in diauxic lag observed when denitrifiers switch from aerobic to anoxic growth was unknown. We have shown that presence of Nap is associated with shorter lags and that deletion of the *nap* operon in one denitrifier greatly increases its diauxic lag. Further work should be carried out to determine the proportions of denitrifiers in different types of nitrogen removing wastewater treatment plants that are Nap-positive. This information could lead to design and operational strategies to enrich the Nap-positive population and thus reduce diauxic lag.

CHAPTER 3
USE OF FLUORESCENCE IN SITU HYBRIDIZATION AS A TECHNIQUE FOR IDENTIFYING NAP$^+$ DENITRIFYING

Introduction

Excess nitrogen discharged in wastewater can cause toxicity and algal blooms in receiving waters. Biological nitrification and denitrification in a single sludge, suspended growth process is a popular method of nitrogen removal from wastewater. In this process, bacteria cycle through oxic and anoxic (no dissolved oxygen, nitrate present) phases. When denitrifying bacteria are transferred from an oxic environment to an anoxic environment, there can be a period of little or no growth (diauxic lag) while denitrifying enzymes are resynthesized.

We have observed that denitrifying bacteria containing periplasmic nitrate reductase (NAP) in addition to membrane-bound nitrate reductase (Nar) have either short or no diauxic lags, whereas those containing only Nar tend to have longer diauxic lags (Casasús et al., 2007). Bacteria can be characterized with regard to presence or absence of NAP using enzyme activity assays. However, these assays are cumbersome and involve hazardous reagents (benzyl-viologen and sodium azide). Alternatively, bacteria can be characterized with regard to the presence of the gene that encodes for NAP (*nap*) by DNA sequencing, which is expensive.

We have constructed a FISH probe for *nap* in order to facilitate identification of bacteria that contain periplasmic nitrate reductase. The probe was tested against two *nap*$^+$ pure cultures (*Paracoccus pantotrophus* ATCC 35512 and *Alcaligenes eutrophus* ATCC 17699) and two *nap*$^-$ pure cultures (*Pseudomonas denitrificans* ATCC 13867 and *Pseudomonas fluorescens* ATCC 17582). Further testing against four isolates of denitrifying bacteria from the University of Florida Water Reclamation Facility was also carried out. The isolates were characterized with regard to presence or absence of NAP using enzyme activity assays and growth studies.

Materials and Methods

Probe Design

The *nap* sequences of four *nap*$^+$ bacteria (*Paracoccus pantotrophus* (NCBI accession number Z36773; Berks et al., 1995), *Alcaligenes eutrophus* (X71385; Siddiqui et al., 1993), *Pseudomonas G-179* (AF083948; Bedzyk et al., 1999), and *Rhodobacter sphaeroides* (AF069545; Bedzyk et al., 1999)) were used to assess the homology of *nap* subunits. The *napA* and *napB* subunits are common to the four bacteria. As the *napA* subunits are longer and have higher complementarity than the *napB* subunits (Table 3-1), we based our probe design on *nap*A.

Table 3-1. Percent homology of *napA* and *napB* subunits in four micro-organisms

Bacterium	*nap* operon	Number of base pairs in *napA*	%Match*	Number of base pairs in *napB*	%Match*
P. pantotrophus	*nap*EDABC	2496		486	
A. eutrophus	*nap*AB	2496	73	510	58
Pseudomonas G-179	*nap*EFDABC	2505	77	492	64
R. sphaeroides	*nap*EFDABC	2496	77	465	65

* In a pairwise comparison to *P. pantotrophus* using Clone Manager Professional Suite Version 8 and the NCBI database.

We searched for homologous regions that met the following criteria: percent G/C content between 50 and 60, a melting temperature between 32 and 100°C, no hairpins, and few repeats (<3), runs(<4) and dimers (<5 adjacent homologous bases). The four longest homologous regions contained 24, 23, 22, and 21 base pairs. For each of these probe candidates, we BLAST searched the NCBI database (http://www.ncbi.nlm.nih.gov/) using the search option "optimized for highly similar sequences (megablast)". The union of the results of the searches was 71 bacteria, out of which 52 contained at least one *nap* subunit (Table 3-2).

The ability of the four candidate probes to bind to the set of 71 bacteria (test set) was evaluated using Clone Manager with the NCBI database. Table 3-3 shows the percent identified

Table 3-2. Bacteria with a highly similar sequence to at least one candidate probe

Organism	Accession number	Subunits of *nap* operon
Cytophaga hutchinsonii ATCC 33406	NC_008255	A
Saccharophagus degradans	NC_007912	ABC
Bordetella parapertussis 12822	NC_002928	CBAD
Bradyrhizobium sp. BTAi1	NC_009485	CBADE
Pseudomonas stutzeri A1501	NC_009434	CBADE
Ralstonia metallidurans CH34	NC_007974	CBADE
Azoarcus sp. BH72	NC_008702	CBADE/CBHGADF
Psychromonas ingrahamii 37	NC_008709	CBADF
Pseudomonas aeruginosa PAO1	NC_002516	CBADFE
Sinorhizobium meliloti 1021 plasmid pSymA	NC_003037	CBADFE
Escherichia coli 536	NC_008253	CBHGA
Escherichia coli O157:H7 str. Sakai	NC_002695	CBHGAD
Rhodobacter sphaeroides ATCC 17025 plasmid pRSPA01	NC_009429	CBHGAD
Salmonella enterica subsp. enterica serovar Choleraesuis str. SC-B67	NC_006905	CBHGAD
Shigella flexneri 5 str. 8401	NC_008258	CBHGAD
Actinobacillus succinogenes 130Z	NC_009655	CBHGADF
Erwinia carotovora subsp. atroseptica SCRI1043	NC_004547	CBHGADF
Escherichia coli APEC O1	NC_008563	CBHGADF
Escherichia coli CFT073	NC_004431	CBHGADF
Escherichia coli O157:H7 EDL933	NC_002655	CBHGADF
Escherichia coli UTI89	NC_007946	CBHGADF
Salmonella enterica subsp. enterica serovar Typhi str. CT18	NC_003198	CBHGADF
Salmonella typhimurium LT2	NC_003197	CBHGADF
Shigella flexneri 2a str. 2457T	NC_004741	CBHGADF
Shigella flexneri 2a str. 301	NC_004337	CBHGADF
Shigella sonnei Ss046	NC_007384	CBHGADF
Hahella chejuensis KCTC 2396	NC_007645	DABC
Bordetella bronchiseptica RB50	NC_002927	EDABC
Bradyrhizobium japonicum USDA 110	NC_004463	EDABC
Bradyrhizobium sp. ORS278	NC_009445	EDABC
Burkholderia xenovorans LB400 Chromosome 3	NC_007953	EDABC
Paracoccus denitrificans	NC_008688	EDABC
Ralstonia eutropha H16	NC_005241	EDABC
Ralstonia eutropha JMP134 chromosome 2	NC_007348	EDABC
Rhodopseudomonas palustris BisB18	NC_007925	EDABC
Shewanella baltica OS185	NC_009665	EDABC
Shewanella loihica PV-4	NC_009092	EDABC
Shewanella baltica OS155	NC_009052	EDABC/DAB

Table 3-2. Continued.

Organism	Accession number	Subunits of *nap* operon
Shewanella amazonensis SB2B	NC_008700	EDABCFDGHB
Agrobacterium tumefaciens str. C58	NC_003063	EFDABC
Pseudomonas aeruginosa PA7	NC_009656	EFDABC
Pseudomonas aeruginosa UCBPP-PA14	NC_008463	EFDABC
Rhodobacter sphaeroides	NC_007489	EFDABC
Sinorhizobium medicae WSM419	NC_009621	EFDABC
Salmonella enterica subsp. enterica serovar Paratyphi A str. ATCC 9150	NC_006511	FAGHBC
Salmonella enterica subsp. enterica serovar Typhi Ty2	NC_004631	FAGHBC
Aeromonas hydrophila subsp. hydrophila ATCC 7966	NC_008570	FDAB
Vibrio cholerae O395	NC_009456	FDABC
Yersinia pseudotuberculosis IP 31758	NC_009708	FDABC
Shigella boydii Sb227	NC_007613	FDAGHBC
Magnetospirillum magneticum AMB-1	NC_007626	HG
Rhodobacter sphaeroides ATCC 17025 plasmid pRSPA02	NC_009430	KEFDABC
Acidobacteria bacterium Ellin345	NC_008009	-
Aeromonas salmonicida subsp. salmonicida A449	NC_009350	-
Anaeromyxobacter sp. Fw109-5	NC_009675	-
Brucella melitensis 16M Chromosome I	NC_003317	-
Burkholderia xenovorans LB400 Chromosome 2	NC_007952	-
Caldicellulosiruptor sacharolyticus	NC_009437	-
Frankia alni ACN14a	NC_008278	-
Halorhodospira halophila SL1	NC_008789	-
Maricaulis maris	NC_008347	-
Mycobacterium gilvum	NC_009338	-
Pelobacter propionicus DSM 2379	NC_008609	-
Pseudoalteromonas atlantica T6c	NC_008228	-
Pseudomonas mendocina ymp	NC_009469	-
Psychrobacter cryohalolentis K5	NC_007969	-
Rhodoferax ferrireducens T118	NC_007908	-
Rubrobacter xylanophilus DSM 9941	NC_008148	-
Sphingomonas wittichii RW1	NC_009507	-
Streptoccus suis 05ZYH33	NC_009442	-
Streptoccus suis 98HAH33	NC_009443	-
Shewanella amazonensis SB2B	NC_008700	EDABCFDGHB
Agrobacterium tumefaciens str. C58	NC_003063	EFDABC
Pseudomonas aeruginosa PA7	NC_009656	EFDABC
Pseudomonas aeruginosa UCBPP-PA14	NC_008463	EFDABC
Rhodobacter sphaeroides	NC_007489	EFDABC

Table 3-3. Performance of candidate probes against the test set of 71 bacteria

Probe candidate	1	2	3	4
Probe length	24	23	22	21
Correct binding	29 (41%)	24 (34%)	60 (85%)	25 (35%)
False positives	1 (1%)	4 (6%)	1 (1%)	0 (0%)
False negatives	41 (58%)	43 (61%)	10 (14%)	46 (65%)

correctly, the percent of false positives and the percent of false negatives. Probe candidates 1, 2, and 4 were considered to be unsuitable because of low percentages of correct identifications and high percentages of false negatives. Probe 3 had low percentages of both false positives and false negatives. Table 3-4 shows the success of each candidate probe in identifying *nap*$^+$ bacteria. Candidate 3 correctly identified 43 of the 52 *nap*$^+$ bacteria.

Our probe design consisted of the sequence of probe candidate 3 with a marker/quencher combination of Fluorescein and DABCYL (Lighton and Fiandaca, 2005). The probe sequence is Fluorescein-5`-GCTCGAACATGGCGGAGATGCA-3`-DABCYL.

Table 3-4. Percent correct identification for *nap* containing bacteria

Probe candidate	Probe length	*nap*$^+$ correctly identified (52 total)
1	24	7 (21%)
2	23	11 (13%)
3	22	43 (83%)
4	21	7 (13%)

Chemicals

All reagents were purchased from Fisher Scientific, Pittsburg PA, unless otherwise specified.

Bacterial Culture

A flask containing125 mL of sterile nutrient broth (Sigma-Aldrich, St. Louis, MO) was inoculated with *Paracoccus pantotrophus* or *Pseudomonas denitrificans* using a sterile inoculating loop. The flask was held at 30˚C with continuous shaking for one day (*P.*

denitrificans) or two days (*P. pantotrophus*). All other strains of bacteria (*Alcaligenes eutrophus*, *Pseudomonas fluorescens*, and four isolates from the University of Florida Water Reclamation Facility) were grown for one day at 37˚C in Luria-Bertani broth with continuous shaking.

Bacterial Isolates

Triplicate samples were taken from the primary anoxic reactor of the University of Florida Biodenipho process and placed in 1-L sterile containers that were pre-incubated in an anaerobic chamber. The samples were kept on ice during transfer to the lab. Samples were centrifuged in 50 mL tubes and the supernatants discarded. Glass beads (20-30) were combined with the pellets and the mixtures vortexed to break up flocs. The deflocculated suspensions were filtered with course sterile filter paper (Whatman Grade 1, pore size 11 μm) and the filtrates were serially diluted with sterile deionized water (10^{-1} to 10^{-8}). To select denitrifying bacteria, 100 μL of each sample dilution was plated in triplicate on PBS-based minimal agar supplemented with nitrate and succinate. The plates were incubated in anaerobic jars at room temperature (20-25 ºC) for 7 days. A total of 72 isolates were obtained, of which four have been characterized with regard to presence or absence of *nap*.

Bacterial Fixation

Fixation of bacteria to glass slides was generally carried out according to Henegariu et al (2000). A 25 mL volume of bacterial suspension was centrifuged at 13000 x g for 10 minutes at 25˚C and the supernatant was poured off. The pellets were suspended in 1 mL freshly prepared 3:1 (v/v) methanol:glacial acetic acid and vortexed until dissolution was complete then transfered to a 1.5 mL micro-centrifuge tube. Cells were washed with the methanol:glacial acetic acid mixture a total of three times - with intermediate centrifugations at 5200 x g for one minute. A volume of 30 μL of treated cell suspension was spread on a sterile glass slide by holding a pipette tip parallel to the surface of the slide while spreading the liquid. As the surface began to

dry and become “grainy”, the slide was passed face down though a steam bath for 1-2 sec, and then placed directly on a hot plate (near maximum heat) for 10 seconds to dry.

The FISH Protocol

The FISH protocol was carried out according to Cancer Genetics Inc (2004). A 70% formamide solution was preheated to 75˚C in a water bath. An ethanol series (70, 80, and 100%) was placed in a freezer at -20˚C, and a second series was left at room temperature. The fixed cells were dehydrated by passing the slide though the room temperature ethanol series; one minute per concentration. The slide was then air-dried for 5 minutes.

The dehydrated bacterial cells were denatured by placing the slide in the warm formamide solution for 2 minutes. It was then immediately passed through the cold ethanol series; one minute per concentration, followed by complete air-drying.

Probe was dissolved in TE buffer to give a concentration of 20 µmol/µL. A volume of 10 µL of probe solution was placed in a 1.5 mL microcentrifuge tube and held in a 80˚C (probe melting temperature =75.5˚C) water bath for 7 minutes to denature the probe. The probe solution was then incubated at 37˚C for 10 minutes and subsequently centrifuged for one minute at 10,600 x g. A volume of 10 µL of denatured probe solution was then applied to fixed bacteria on the slide and covered with a coverslip. The slide was stored overnight (16-18 hours) at 37˚C.

After overnight storage, the coverslip was removed and the slide was immersed for 5 minutes in a 45˚C solution of 0.5x sodium saline citrate/0.1% w/v SDS solution. The slide was transferred to a second 0.5x SSC/0.1% SDS solution for another 5 minutes at the same temperature. The slide was next rinsed with DI water and allowed to air-dry. Finally, the slide was covered with a second coverslip and viewed under an epifluorescent microscope using 10x ocular and a 100x or 60x objective lens.

Nitrate reductase assays (Casasús et al., 2007 and Hamilton et al., 2005) were carried out on biomass samples taken before the switch from aerobic to anoxic conditions and after the resumption of exponential growth in the anoxic phase. Parallel enzyme assays were carried out with and without sodium azide, which is an inhibitor of Nar. The activity in the presence of azide was subtracted from the activity in the absence in the azide to obtain the Nar activity. The NAP activity is represented by the activity measured in the presence of azide. Lengths of diauxic lags exhibited during growth of the bacteria were calculated according to Lee et al (2008, in press).

Results and Discussion

The fixed *nap*$^+$ pure cultures fluoresced under UV light, whereas the *nap*$^-$ pure cultures showed no fluorescence. For example, Figures 3-1 and 3-2 show *P. pantrotrophus* (a *nap*$^+$ bacterium) under incandescent and epifluorescent light respectively. The bacteria visible under incandescent illumination are also visible under epifluorescent illumination, indicating that the probe hybridized with these bacteria. In contrast, the *nap*$^-$ *P. denitrificans* are not visible under epifluorescent illumination (Figure 3-4) but are visible under incandescent illumination (Figure 3-3) indicating the prode did not hybridize. The other two pure cultures, the *nap*$^+$ *A. eutrophus* and the *nap*$^-$ *P. fluorescens* also tested correctly with the probe, with only *A. eutrophus* fluorescing.

To further test the probe, we obtained isolates from the University of Florida Water Reclamation Facility and determined whether or not they were *nap*$^+$ using enzyme assays. The assay results measured during anoxic growth, after an initial aerobic growth period, are shown in Table 3-5. Isolates KJ13 and KJ72 exhibited significant NAP activity, whereas isolates KJ14 and

Figure 3-1. *Paracoccus pantotrophus* viewed at 600x magnification under incandescent light.

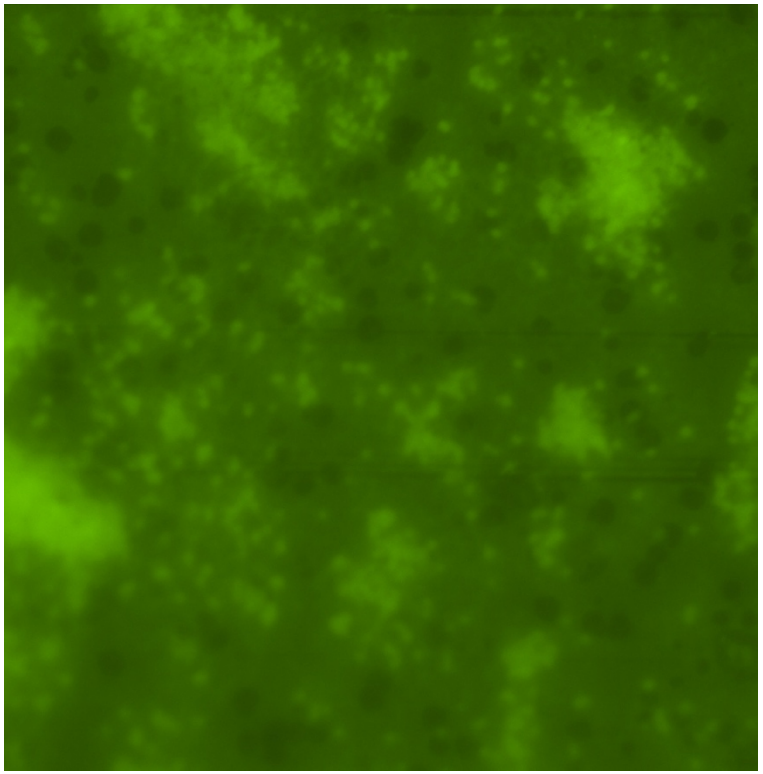

Figure 3-2. *Paracoccus pantotrophus* viewed at 600x magnification under UV light after being treated with fluorescent probe that targets *napA*.

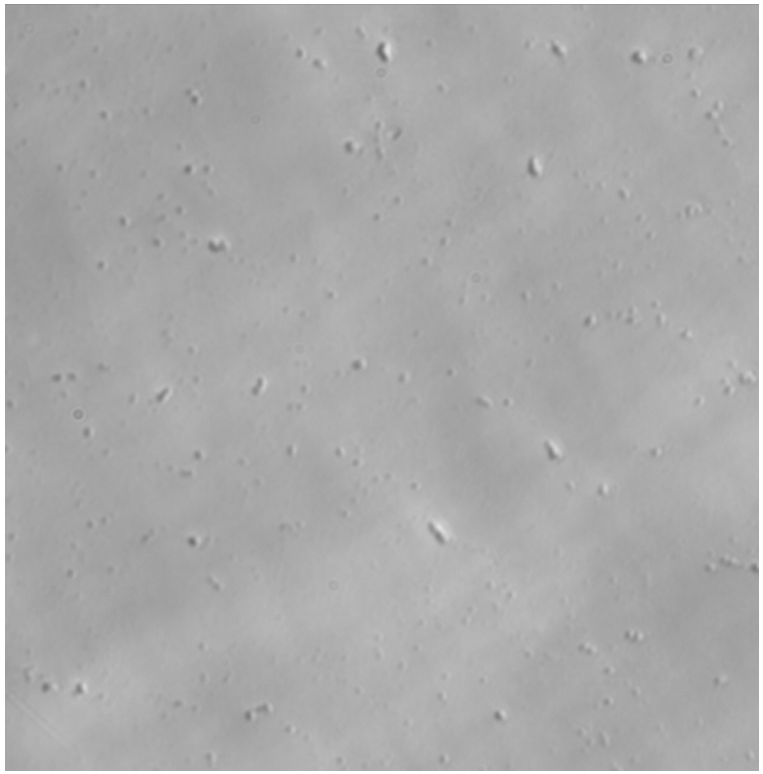

Figure 3-3. *Pseudomonas denitrificans* viewed at 600x magnification under incandescent light.

Figure 3-4. *Pseudomonas denitrificans* viewed at 600x magnification under UV light after being treated with fluorescent probe.

Table 3-5. Enzyme activity data and diauxic lag lengths compared to probe results

Isolate	Diauxic lag (hr)	Before anoxic switch		Presence of Nap
		Nar	Nap	
KJ013	2.17	0.27 ± 0.10	0.25 ± 0.10	Yes
KJ014	> 14	0.65 ± 0.10	0.08 ± 0.04	No
KJ070	>10	4.04 ± 1.55	0.35 ± 0.37	No
KJ072	1.38	0.33 ± 0.17	0.56 ± 0.05	Yes

KJ70 had near zero levels of NAP activity. Measurements of diauxic lag (Table 3-5) show short lags for the first two isolates, compared to long lags for the second pair of isolates. Based on these results, we conclude that the first pair of isolates are *nap*$^{+}$ and the second pair of isolates are *nap*$^{-}$. The probe assays show the first two isolates as fluorescing while the second pair of isolates did not fluoresce.

After establishing probe efficacy we used it to characterize a sample of activated sludge taken from the primary anoxic reactor of the University of Florida Water Reclamation Facility. Figure 3-6 shows that a significant portion of bacteria in the sample studied contained *nap*.

To our knowledge, this is the first time a DNA probe has been developed for identifying *nap*$^{+}$ bacteria. The probe successfully identified four pure cultures and four isolates. Application of the probe to a waste water microbial population indicated a significant proportion of *nap* containing bacteria. Use of this probe in conjunction with population sampling and pilot plant studies can lead to better understanding of the role of *nap*$^{+}$ bacteria in wastewater denitrification.

Figure 3-5. Bacteria isolated from the University of Florida Waste Water treatment plant viewed at 600x magnification under incandescent light.

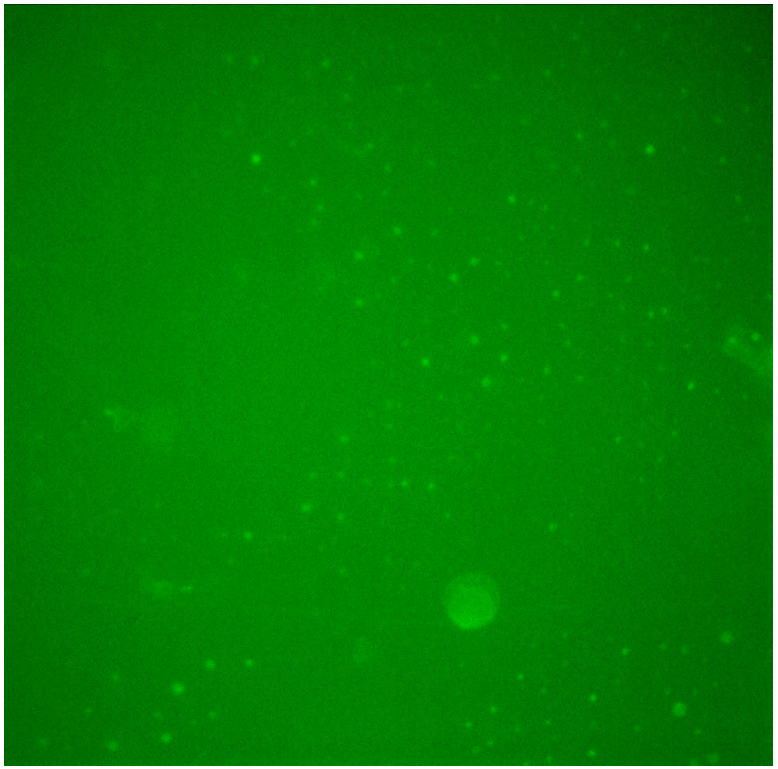

Figure 3-6. Bacteria isolated from the University of Florida Water Reclamation Facility viewed at 600x magnification under UV light after being treated with fluorescent probe that targets *napA*.

CHAPTER 4
DIAUXIC GROWTH MODEL BASED ON NAP AND NAR SYNTHESIS KINETICS FOR DENITRIFYING BACTERIA

Introduction

Nitrate removal is an important component of advanced wastewater treatments plants. Nitrogen is commonly removed by biological means because they are both efficient and cost effective (Grady et al., 1999). Bacteria mediated nitrogen removal in wastewater treatment plants occurs through oxidation of ammonia to nitrate (nitrification) and reduction of nitrate to nitrogen gas (denitrification). Since oxygen respiration is more energetically favored than denitrification, facultative bacteria usually utilize nitrogen oxides only in the absence of oxygen (Oh and Silverstein, 1999b).

In a typical biological nitrogen removal system, biomass is exposed to alternating cycles of aerobic and anoxic phases to maximize the removal of nitrate (Ramalho, 1983). This may result in a diauxic lag. Diauxie or biphasic growth is characterized by a period of little or no growth in between two exponential growth phases. This occurs when bacteria switch from oxygen to nitrate as electron acceptors and it corresponds to the period during which the cell has to produce the necessary enzymes to respire on the less preferred substrate. Monod (1942) was first to characterize diauxic lag due to change in electron donors. Biphasic growth due to a change in electron acceptors (nitrate to nitrite) was first studied by Kodama et al (1969). Later many investigators (Waki et al., 1980; Liu et al., 1998a, 1998b; Gouw et al., 2001; Lisbon et al., 2002; Casasús et al., 2007) have shown that when bacteria change from dissolved oxygen to nitrate as terminal electron acceptor, there can be encountered by the phenomenon of diauxic lag. Diauxic lags are undesirable as they reduce the overall rate of nitrate removal.

Commonly used Activated Sludge Models (ASM) 1, 2, 2d and 3 (Henze et al., 2000) do not capture diauxic lag. Liu et al (1996, 1998a) extended ASM-1 so that it can portray diauxic

lag in activated sludge systems when the terminal electron acceptor switches from oxygen to nitrate. Later Liu et al. (1998b) modified their model so that it can predict the extension of lag phase that was observed when the length of the preceding aerobic phase was increased.

Hamilton et al (2005) modeled diauxic lag observed in *Pseudomonas denitrificans* by considering the intracellular variables as well as the substrate concentrations in the solution. They assumed the presence of a nitrate respiration operon and that nitrate reductase and the nitrate transport protein are synthesized together. They linked the nitrate reductase enzyme synthesis to the active nitrate transport into the cell and considered the effect of overall enzyme synthesis kinetics on anoxic growth.

Dissimilatory nitrate reduction is carried out by membrane bound nitrate reductase (Nar) under anoxic condions. Nar is believed to be present in all denitrifies. However some denitrifiers also have the second dissimilatory nitrate reductase – periplasmic nitrate reductase (Nap). It has been suggested that Nap may be utilized in the adaptation to metabolism in the absence of oxygen after transition from aerobic conditions (Moreno-Vivián et al., 1999). It has been observed that bacteria that have both Nap and Nar have shorter diauxic lags when compared to bacteria that have only Nar (Casasús et al., 2007; Durvasula et al., in print). Durvasula et al (in print) attribute shorter diauxic lags to the presence of Nap.

In this work, we extend Hamilton et al. (2005) model to bacteria that have both of the nitrate reductase enzymes.

Model

The enzyme synthesis model described by Hamilton et al (2005) is adapted to include periplasmic nitrate reductase (Nap) synthesis kinetics.

Rate of Synthesis of Nar

The cell takes up nitrate from the environment under anoxic conditions. The internal nitrate induces the synthesis of Nar. This allows growth anoxically and promotes further nitrate uptake. The rate of synthesis of Nar is denoted by r_{en_nar}. The model used is that of a single effector molecule binding to a single repressor molecule (Yagil and Yagil, 1977; Hamilton et al., 2005). K_1 is the equilibrium constant for the binding of repressor to internal nitrate (inducer molecule) and K_2 is the constitutive rate of enzyme synthesis which is a function of equilibrium constant for the binding of repressor to operator. The organic substrate dependence of Nar is captured by the Monod term.

$$r_{en,nar} = a_{N,nar}\left(\frac{1+K_1 s_{ni}}{K_2 + K_1 s_{ni}}\right)\left(\frac{S_s}{K_{s,an} + S_s}\right) \tag{4-1}$$

Here s_{ni} denotes the concentration of nitrate inside the cell, S_s is the carbon substrate concentration.

Rate of Synthesis of Nap

Periplasmic nitrate reductase (Nap) is synthesized under aerobic conditions, but can operate in either the presence or absence of oxygen. Synthesis of Nap is unaffected by the presence of nitrate or ammonia (Moreno-Vivián et al., 1999). The fact that the periplasmic enzyme is present in anaerobically grown cells accounts for their capacity for aerobic nitrate reduction (Bell et al., 1990). The effect of oxygen and of carbon substrate on the synthesis of Nap are portrayed by Monod terms. The rate of synthesis of Nap, r_{en_nap} is described by Equation (4-2).

$$r_{en,nap} = a_{N,nap}\left(\frac{S_O}{S_O + K_{OH}}\right)\left(\frac{S_s}{K_{s,ox} + S_s}\right) \tag{4-2}$$

Oxic Growth

The rate of oxic growth is based on the kinetic expression of Hamilton et al (2005).

$$r_{ox} = \mu_{max,ox}\left(\frac{S_O}{S_O + K_{OH}}\right)\left(\frac{S_s}{K_{s,ox} + S_s}\right) \tag{4-3}$$

Specific Rate of Nitrate Uptake

The rate of nitrate uptake is proportional to the concentration of membrane bound nitrate reductase (e_{nar}) similar to the approach adopted by Shoemaker et al (2003) for modeling diauxic lag when switching carbon sources. Oxygen represses the synthesis of the membrane-bound dissimilatory nitrate reductase (Warnecke-Eberz and Friedrich, 1993; Moreno-Vivian et al., 1999) at the level of nitrate transport (Berks et al., 1994). A Monod term for the substrate is included to explain the energy dependence of nitrate uptake.

$$r_{sni} = V_{sni}\left(\frac{e_{nar}}{e_{nar,max}}\right)\left(\frac{K_{Oi}}{S_{Oi} + K_{Oi}}\right)\left(\frac{S_s}{K_{s,an} + S_s}\right)\left(\frac{S_N}{K_{NOi} + S_N}\right) \tag{4-4}$$

Anoxic Growth

Anoxic growth is proportional to concentration of membrane bound nitrate reductase (e_{nar}). The rate of nitrate uptake influences the synthesis of Nar, thereby affecting anoxic growth. Like Hamilton et al (2005) we have not included a term for oxygen inhibition of nitrate transport as the inhibitory term is included in the nitrate uptake kinetics. Due to the periplasmic location of Nap, some denitrifiers carry out aerobic denitrification (Bell et al., 1990). Since no transport of nitrate is required, nitrate from the environment can be utilized by Nap. In *Pseudomonas G* -179, Nap was found to catalyze the first step of denitrification (Bedzyk et al., 1999). We assume that at the onset of anoxic growth, the Nap that was synthesized aerobically initiates denitrification thereby contributing to anoxic growth and short diauxic lag. Denitrification due to Nap is dependent on concentration of periplasmic nitrate reductase (e_{nap}) and the nitrate in the

environment. As Nar builds up inside the cell, denitrification due to Nar is more energetically preferred to that of Nap. η is the ratio of maximum growth that can be achieved on only Nap to the growth on both Nap and Nar.

$$r_{anox} = \mu_{max,anox}\left(\frac{S_s}{K_{s,an}+S_s}\right)\left[(1-\eta)\left(\frac{e_{nar}}{e_{nar,max}}\right)\left(\frac{s_{ni}}{s_{ni,max}}\right)+\eta\left(\frac{e_{nap}}{e_{nap,max}}\right)\left(\frac{S_N}{S_N+K_N}\right)\right] \tag{4-5}$$

For the model, the specific biomass decay rate (b) is assumed to be constant. The same specific enzyme decay rate (b_{NO}) is asuumed for both nitrate reductases (Nap and Nar. It is also assumed to be constant. The mass balance on the reactor using the above rates yields the equations.

$$\frac{dX_B}{dt} = (r_{ox}+r_{anox}-b)X_B \tag{4-6}$$

$$\frac{dS_s}{dt} = \left(-\frac{1}{Y_{c,ox}}r_{ox}-\frac{1}{Y_{c,an}}r_{anox}\right)X_B \tag{4-7}$$

$$\frac{dS_N}{dt} = -r_{sni}X_B \tag{4-8}$$

$$\frac{de_{nar}}{dt} = r_{en.nar}-\left(b+b_{NO}+\frac{1}{X_B}\frac{dX_B}{dt}\right)e_{nar} \tag{4-9}$$

$$\frac{de_{nap}}{dt} = r_{en.nap}-\left(b+b_{NO}+\frac{1}{X_B}\frac{dX_B}{dt}\right)e_{nap} \tag{4-10}$$

$$\frac{ds_{ni}}{dt} = r_{sni}-\nu_{N,an}r_{anox}-\left(b+\frac{1}{X_B}\frac{dX_B}{dt}\right)s_{ni} \tag{4-11}$$

In Equations 4-9, 4-10 and 4-11 the last term represents dilution due to growth and cell decay (Hamilton et al., 2005). The theoretical maximum values of s_{ni}, e_{nar} and $e_{nap,}$ are found by

setting their respective derivatives to zero and assuming non-limiting concentrations of substrate and nitrate.

$$s_{ni,max} = \frac{V_{sni}}{\mu_{max,anox}} - \nu_{N,an} \tag{4-12}$$

$$e_{nar,max} = \frac{a_{N,nar}}{b + b_{NO}} \left(\frac{1 + K_1 s_{ni,max}}{K_2 + K_1 s_{ni,max}} \right) \tag{4-13}$$

$$e_{nap,max} = \frac{a_{N,nap}}{b + b_{NO}} \tag{4-14}$$

The intracellular variables s_{ni} (mg/gdw), e_{nar} (mol BV/gdw.hr) and e_{nap} (mol BV/gdw.hr) are expressed per gram dry weight. The extracellular components X_B (gdw/L), S_s (mg/L) and S_N (mg/L) are expressed in volumetric concentrations. The dissolved oxygen concentration (S_O) was assumed to near saturation under aerobic conditions and zero under anoxic conditions.

Materials and Methods

Paracoccus pantotrophus (ATCC 35512) was chosen for the experiments since it has both nitrate reductase enzymes Nap and Nar. A mutant of *P. pantotrophus* (Durvasula et al., in print) lacking in Nap was also cultured and the fitted model was tested against the experimental values of biomass and enzyme acitivity for both organisms.

Growth Experiments

The preculture of *P. pantotrophus* (ATCC 35512) and the mutant of *P. pantotrophus* deficient in Nap were cultured in LB (Luria-Bertani) broth supplemented with 400 mg $NO_3^- - N$ / L for 12-18 hr at 37°C in a shaking incubator. The biomass from the preculture was used to inoculate a 1 L fresh, autoclaved solution of LB supplemented with nitrate (400 mg $NO_3^- - N$ / L) in a fermentor (Bio Flo 2000, New Brunswick Scientific New Brunswick, NJ) at

an absorbance of 0.1-0.11 (34 – 37.4 gdw/L) at 550nm. The fermentor was stirred at 200 rpm and temperature was maintained at 37°C. During the aerobic phase, air was supplied to the fermentor at a rate of 3 L/min. Air was humidified by a bubbling through a flask of autoclaved, deionized water and filtered by passing through 0.3 μm Whatman Hepa-Vent Glass microfiber filters in series. The growth of the bacteria in the fermentor was monitored by absorbance measurements taken every 30 -45 minutes at 550nm in Thermo-Spectronic Genesys 10UV spectrophotometer. Aerobic growth was carried out till the biomass reached exponential phase. Then the fermentor was switched to anoxic growth by replacing air by nitrogen gas. The experiment was continued anoxically till the culture reached exponential phase. Enzyme assays were done just before switch to the anoxic phase and once during the anoxic exponential growth phase. The assays were carried out as described by Hamilton et al (2005) and Casasús et al (2007) for calculation of periplasmic and membrane bound nitrate reductase activities.

Optimization

The optimization technique called "Differential Evolution" (Price and Storn, 1997) was used for optimizing the model parameters to fit the simulation results to the experimental values. The objective function was formulated so as to minimize the squared relative error between the measured concentration of biomass and concentration of biomass predicted by the model as well as squared relative error of the enzyme activity measurements at those time points where data was available.

$$C = \frac{\sum_{i=1}^{N}\left(X_{B,predicted} - X_{B,measured}\right)^2}{X^2_{B,av,measured}} + \frac{\left[\left(e_{nar,predicted} - e_{nar,measured}\right)^2_{aerobic} + \left(e_{nar,predicted} - e_{nar,measured}\right)^2_{anoxic}\right]}{e^2_{nar,av,measured}} + \frac{\left[\left(e_{nap,predicted} - e_{nap,measured}\right)^2_{aerobic} + \left(e_{nap,predicted} - e_{nap,measured}\right)^2_{anoxic}\right]}{e^2_{nap,av,measured}}$$

(4-15)

All the reaction kinetic equations, rate equations and objective function for the optimization mentioned in equation 4-15 are for the *P. pantotrophus* which has both the nitrate reductases, Nap and Nar. In case of the mutant which lacks Nap, the equations written for Nap and the terms for Nap in all the other equations mentioned thus far were set to zero.

The parameters estimated are $\mu_{max,ox}$, $\mu_{max,anox}$, $K_{s,ox}$, $K_{s,an}$, K_{OH}, K_{Oi}, K_{NOi}, K_N, b, b_{NO}, $Y_{c,ox}$, $Y_{c,an}$, $\nu_{n,an}$, K_1, K_2, $a_{N,nap}$, $a_{N,nar}$, V_{sni} and η. The initial enzyme activities were also fitted. The value of S_O was taken to be 8mg/L under aerobic conditions and zero once the biomass was switched to anoxic phase.

Results and Discussion

The model was first fit to the experimental data of *Paracoccus pantotrophus* (wild-type) since it has both nitrate reductases. The model captured the exponential phases in both aerobic and anoxic phases and the short diauxic lag exhibited by the wild-type (Figure 4-1). The parameters obtained after fitting are listed in Table 4-1.

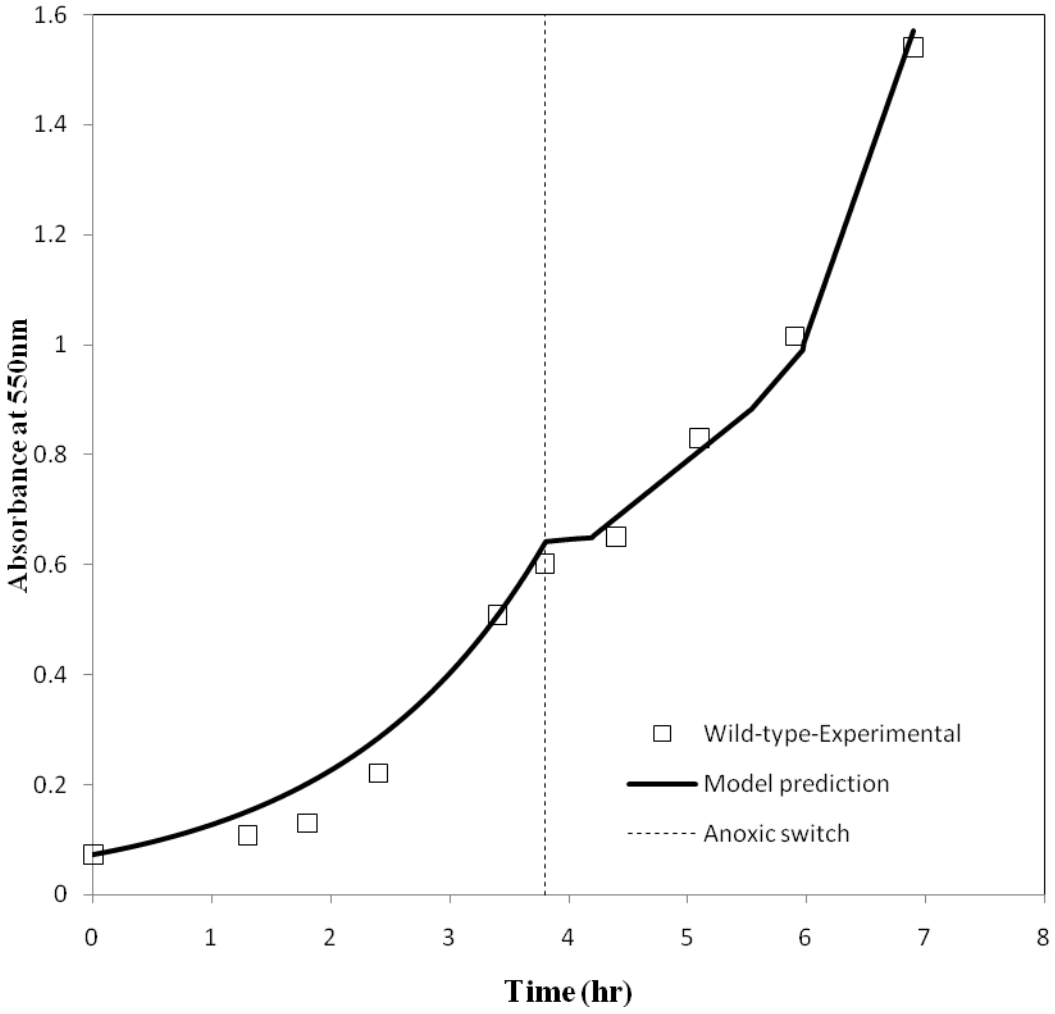

Figure 4-1. Model fit to the fermentor growth data of *P. pantotrophus*.

Good model fits were obtained for the mutant. This model captured the long diauxic lag exhibited by the mutant.

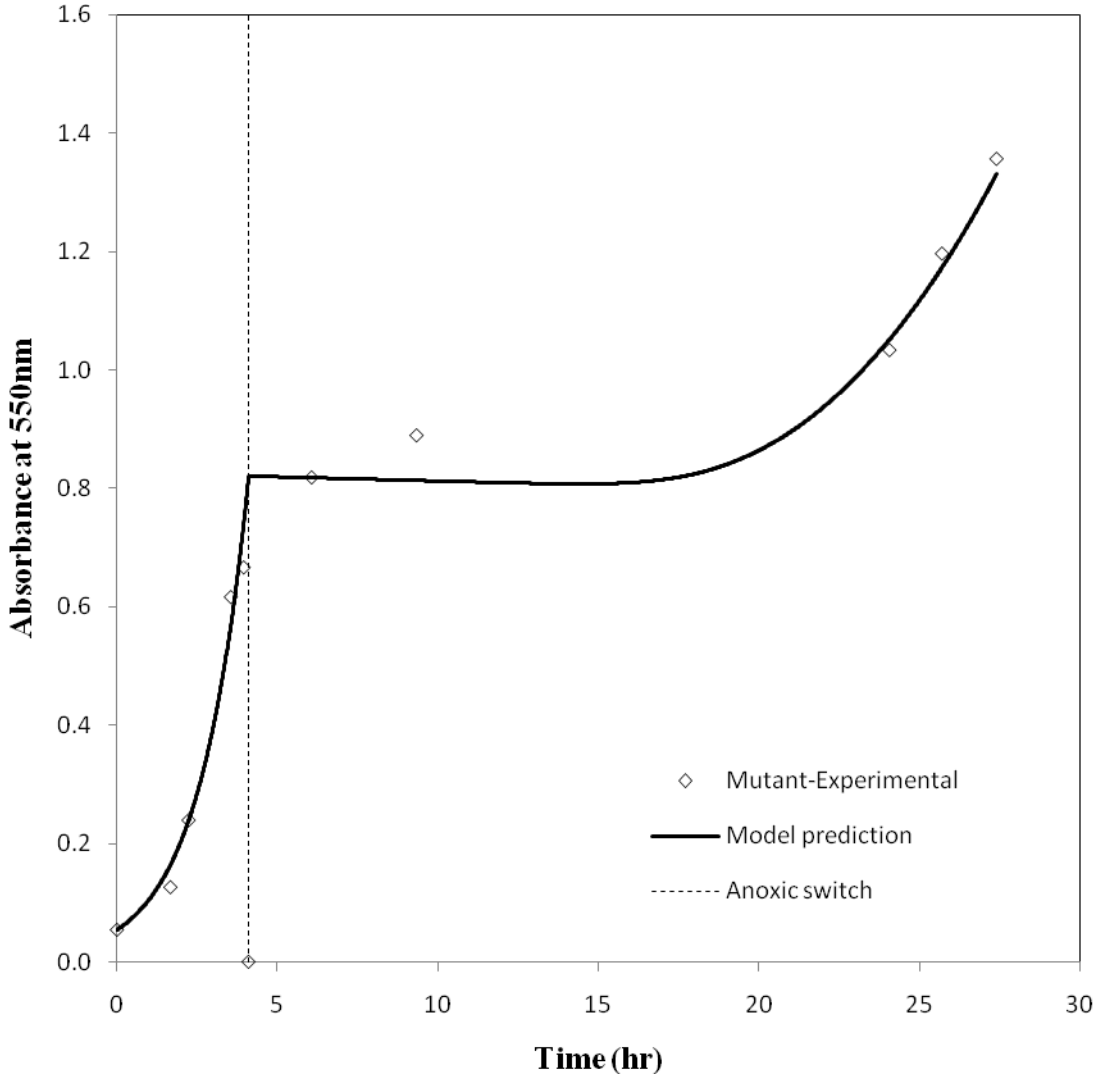

Figure 4-2. Model fit to the fermentor growth data of the mutant

Table 4-1. Parameter values obtained after fitting.

Parameter	Units	Wild-type	Mutant
$K_{s,ox}$	mg substrate/L	0.080	0.080
$K_{s,anox}$	mg substrate/L	1.596	1.596
K_{OH}	mg oxygen/L	2.509	2.509
K_{Oi}	Mg oxygen/L	5.985	5.985
K_{NOi}	mg nitrate/L	2.155	2.155
K_N	mg nitrate/L	0.863	-
b	1/hr	0.002	0.002
b_{NO}	1/hr	1.561	1.561
$Y_{c,ox}$	mg biomass/mg substrate	0.919	0.919
$Y_{c,anox}$	mg biomass/mg substrate	0.953	0.953
$\nu_{N,an}$	mg nitrate/gdw biomass	0.226	0.226
K_1	gdw biomass/mg nitrate	9.980E+24	9.980E+24
K_2	-	9.630E+23	9.630E+23
$a_{N,nap}$	mol BV/gdw biomass.hr^2	6.710E-06	-
$a_{N,nar}$	mol BV/gdw biomass.hr^2	2.020E-05	2.020E-05
V_{sni}	mg nitrate/gdw biomass.hr	0.065	0.065
η	-	0.460	-
$\mu_{max,ox}$	1/hr	0.714	0.875
$\mu_{max,anox}$	1.hr	0.149	0.099
$e_{nar,initial}$	mol BV/gdw biomass.hr	7.000E-08	3.050E-07
$e_{nap,initial}$	mol BV/gdw biomass.hr	6.410E-08	-

CHAPTER 5
FUTURE WORK

Introduction of *nap* Gene in a Nap-Deficient *Pseudomonas denitrificans*

In the present work, we showed that presence of periplasmic nitrate reductase (Nap) is a determining factor in shortening the length of the diauxic lag (Chapter 2). It will be interesting to check if the converse would be true if we followed the opposite approach to what we did in Chapter 2. That is to introduce a plasmid containing the *nap* gene into an organism, like *Pseudomonas denitrificans*, which doesn't have this gene. To accomplish this objective we need to first select a suitable plasmid that is compatible with the host *P. denitrificans*. The plasmid should be able to replicate in the host. *nap* gene along with the *nap* promoter from *Paracoccus pantotrophus* should be cloned to the plasmid with selectable markers and should be transformed into *P. denitrificans*. If the host polymerase doesn't recognize the *nap* promoter of *P. pantotrophus*, we need to construct another plasmid with a different promoter like *lac*. Growth experiments described in Chapter 2 should be carried out for both the wild-type and the new organism harboring the plasmid. Enzyme assay measurements should be carried out in aerobic and anoxic exponential phases to determine the nitrate reductase activities for both species. It is important to know if the levels are in accordance with the trends usually observed. This will confirm the proper regulation of Nap. If the resulting lag has decreased for the new organism, this will further strengthen our theory about the effect of Nap on diauxic lag. This will also give us evidence that *nap* can form a functional protein even in a Nap-deficient bacterium. It will be interesting to check if the location of Nap in the newer organism is same as in a Nap-positive bacterium, which is in the periplasmic space. The increase in reduction state of carbon substrate increases the activity of Nap (Ellington et al., 2002). Casasús et al (2007) reported that with the increase in reduction state of the carbon, the length of the lag decreases. Growth experiments

with different carbon substrates should be carried out and should be tested for the activity of Nap. If the results match with the reported values, it will further provide evidence for proper functioning of Nap.

Construction of Nar Probe using FISH

The ability of facultative bacteria to respire on nitrate is attributed to the function of membrane bound nitrate reductase (Nar). Nar takes electrons from the quinol pool to reduce nitrate to nitrite. In a nitrate removing wastewater treatment plant, it will be beneficial to know what proportion of the bacteria in the activated sludge are denitrifiers. Since all denitrifiers have the membrane bound nitrate reductase, Nar (Moreno-Vivián et al., 1999), the presence of Nar can be used as a tool for their identification.

The subunit composition of Nar may vary from organism to organism. The first step towards construction of the probe is to find the subunit that is common to most organisms. The percent homogeneity of that subunit amongst the different organisms should be checked as this will determine if a probe construction is possible or not. Probes of different lengths should be BLAST searched against the NCBI website, to determine the number of false positives and false negatives. The probe with the highest percentage of correct identification of Nar should be selected as the probe for Nar.

The protocol for FISH (Fluorescence in situ hybridization) explained in Chapter 3 should be carried out for the Nar probe. First pure cultures of the denitrifiers (*Paracoccus pantotrophus, Pseudomonas denitrificans, Alcaligenes eutrophus, Pseudomonas fluorescens)* must be tested to check the efficiency of the probe. The detection of a signal under the light confirms the presence of Nar. The use of the probe on a sample from the denitrification unit of the wastewater treatment plant will give us idea about the percentage of denitrifiers. This knowledge can help in

increasing the plant's nitrate reduction rate by devising strategies that increase the proportion of denitrifiers.

Colony Hybridization

Fluorescence in situ hybridization (FISH) is very useful detection technique in determining the presence or absence of a particular trait. We have isolated 72 species from the denitrifying unit of Water Reclamation facility of University of Florida, Gainesville. We need to find which of these isolated have the periplasmic nitrate reductase (Nap). FISH should be carried out separately for each one of these isolates which makes it cumbersome and very time consuming. In cases such as these, colony hybridization may be the answer.

In colony hybridization, a large number of colonies can be screened simultaneously to determine the presence of a particular DNA sequence or a gene. The colonies to be screened are first cultured on a suitable agar medium. They are then transferred onto a nitrocellulose membrane after marking the reference point on both the agar plate and membrane. The cells on the membrane are lysed and the DNA is denatured. A fluorophore labeled probe for the gene of interest is added to the denatured DNA. After allowing for hybridization, the membrane is washed to rinse out the unbound probe. A UV light is shined on the membrane containing the colonies. The colonies that glow are those which have the gene of interest. By comparing the location of those colonies which glowed under UV to those on the master plate, we will know which isolate has the gene (Grunstein and Hogness, 1975).

Effect of the Carbon Substrate Reduction State on the Length of the Diauxic Lag

The length of the diauxic lag depends on the reduction state of the carbon substrate (Casasús et al., 2007). Better mathematical models must be developed which not only takes into

consideration enzyme synthesis but also the dependence of it on the reduction state of the carbon. This will give us a better insight into the denitrification process and also aid in predicting lag lengths.

APPENDIX A

GENE DELETION STRATEGY

Step 1: Culture *E coli* Containing Helper Plasmid

Materials

pRK2073 in *E. coli* DF 1020
LB broth and LB agar plates

Procedure

- pRK2073 in *E. coli* was cultured in LB medium for a 24 hrs at 37˚C aerobically and plated out on LB agar medium.

- A colony was picked out from the plates and again cultured in LB medium for 24 hrs at 37˚C aerobically and again plated out on LB agar medium. A colony out of these plates was used in triparental mating.

Step 2: PCR Amplification Kanamycin Resistance Gene from pACYC177 using Primers with *EcoR*I/ *Sph*I Restriction Sites

Materials

Taq PCR mastermix
Forward and reverse primers
pACYC177
PCR tubes
Thermal Cycler
Bromophenol blue dye with 40% sucrose
λ/*Hind* III marker

Procedure

- The reaction for PCR was set up in 0.2 mL PCR tube (Table A-1).

- The tube was then placed in a thermal cycler. The annealing temperature was set to be 5˚C less than the melting temperature of the primers and the extension time was based on 1kb/1min calculation.

- Gel electrophoresis was used for confirming the PCR product. 0.8% agarose stained with ethidium bromide was charged with PCR product (5.0 μL of PCR product and 5.0 μL of 1X dye) in one well and λ/*Hind* III marker in the other well.

- DNA was precipitated using the standard procedure. Sodium acetate (pH 5.2) was added to a final concentration of 0.3M from a 3M stock and mixed well. 2 volumes of 95% ethanol was added and incubated at 0˚C for 1 hour before centrifuging down for 15 min at

15,000g. The supernatant was removed and DNA was washed with 0.5mL of 70% alcohol. The contents were centrifuged for 15 min, the supernatant was removed and ethanol was blot dried. The pellet was air dried for 10 min. The DNA was dissolved in 25 μL of deionized H_2O and was stored at -20˚C for further use.

Table A-1. PCR reaction ingredients

Reaction Mixture	Volume (μL)
PCR Mastermix	25
Water	22
Forward primer (200 μM)	1.0
Reverse primer (200 μM)	1.0
Template DNA (pACYC177)	1.0
Total Volume	50

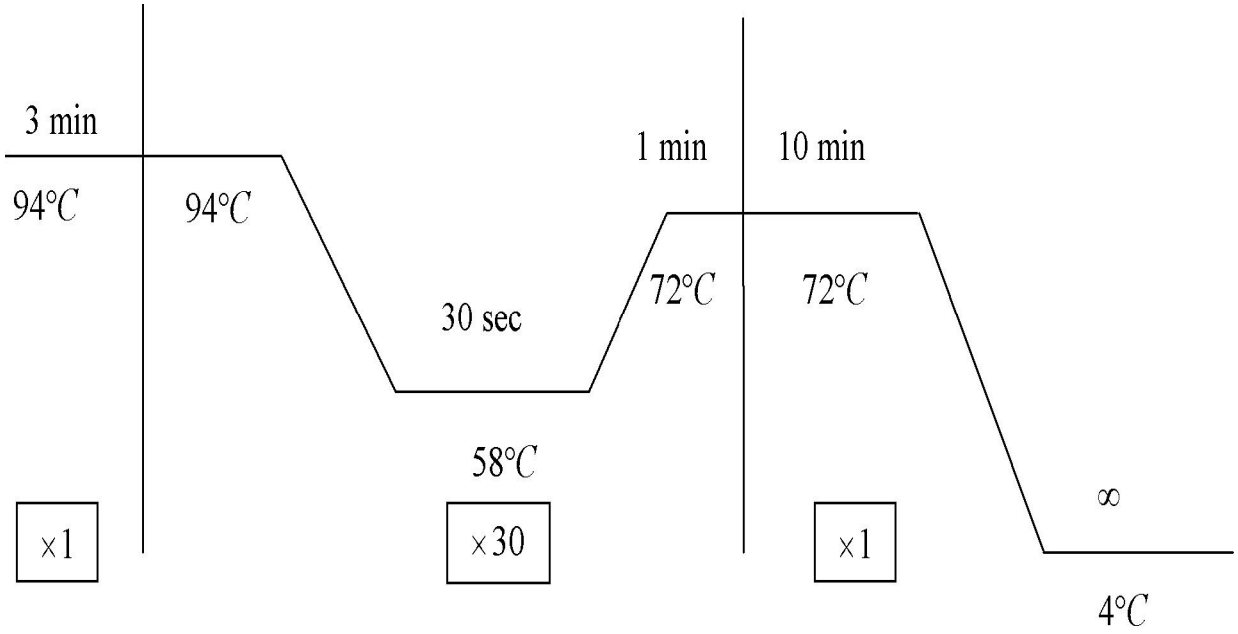

Figure A-1. The PCR temperature profile used.

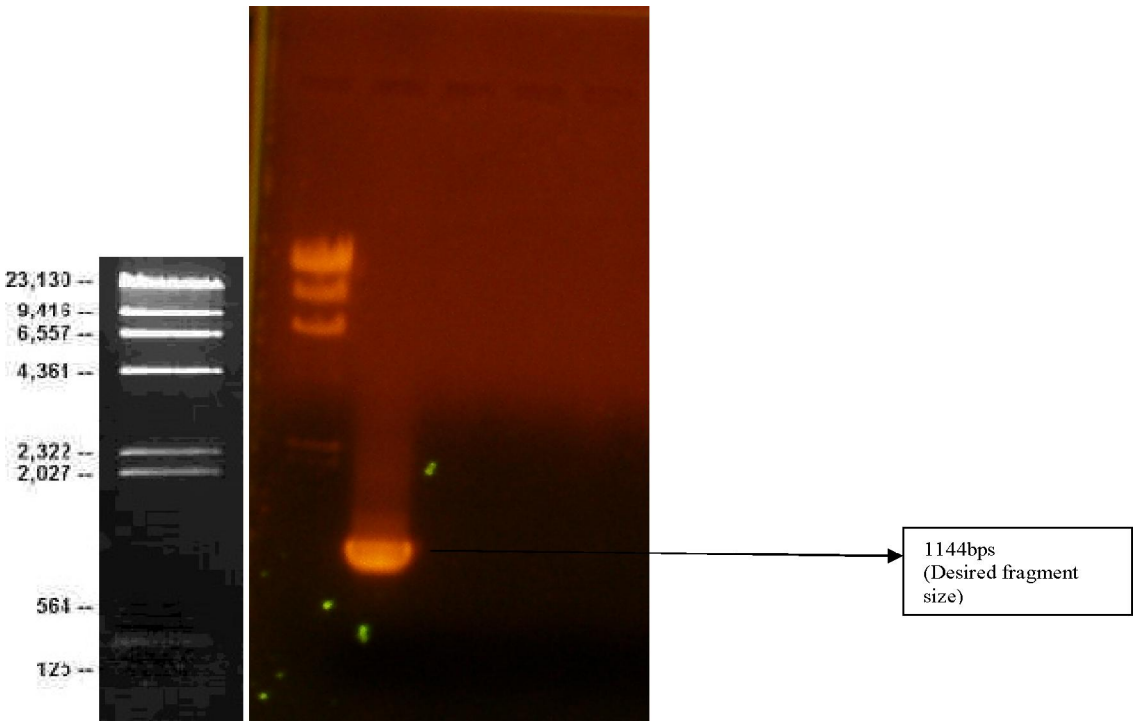

Figure A-2. Gel picture: desired fragment size

Step 3: Clone PCR Fragment in pRVS1

Materials

PCR fragment
*EcoR*I and *Sph*I restriction enzymes
pRVS1
10X NEBuffer EcoRI
DNA ligase (T4)

Procedure

- PCR amplified DNA and pRVS1 was digested with *EcoR*I and *Sph*I restriction enzymes (Table A-2) for an hour at 37˚C (Table A-2).

- The reaction mixture was incubated at 16˚C for 2 hours. The resulting plasmid was the donor plasmid (Table A-3).

Table A-2. Double digest reaction set up

Reaction Mixture	Volume (μL)
Buffer (10X)	1.5
DNA (PCR fragment or pRVS1)	2.0
*EcoR*I	0.5
*Sph*I	0.5
Water	10.5
Total Volume	15.0

Table A-3. Ligation reaction

Reaction Mixture	Volume (μL)
10X ligation buffer	3.0
Insert DNA (PCR fragment)	15.0
Vector DNA (from pRVS1)	12.0
DNA ligase	0.5
Total Volume	30.5

Step 4: Transformation of Donor Plasmid into Donor *E. coli*

Materials

Donor plasmid
LB + kKanamycin
E.coli DH5α (Competent cell)
SOC Medium

Procedure

- A tube of competent *E. coli* cells was thawed on ice for 10 minutes.
- 5 μL containing of pKD100 was added to the cell mixture. The tube was flicked 4-5 times to mix cells and DNA.
- The mixture was placed on ice for 30 minutes. It was heat shocked at exactly 42°C for exactly 30 seconds. It was placed on ice for 5 minutes.
- 250 μL of room temperature SOC was added into the mixture.
- It was placed in a shaking incubator at 37°C, 250 rpm for 60 minutes.
- The cells were thoroughly mixed by flicking the tube and inverting. Several 10-fold serial dilutions were performed in SOC.
- 100 μL of each dilution was plated onto warm selection plates (LB + kanamycin) and incubated overnight at 37°C.

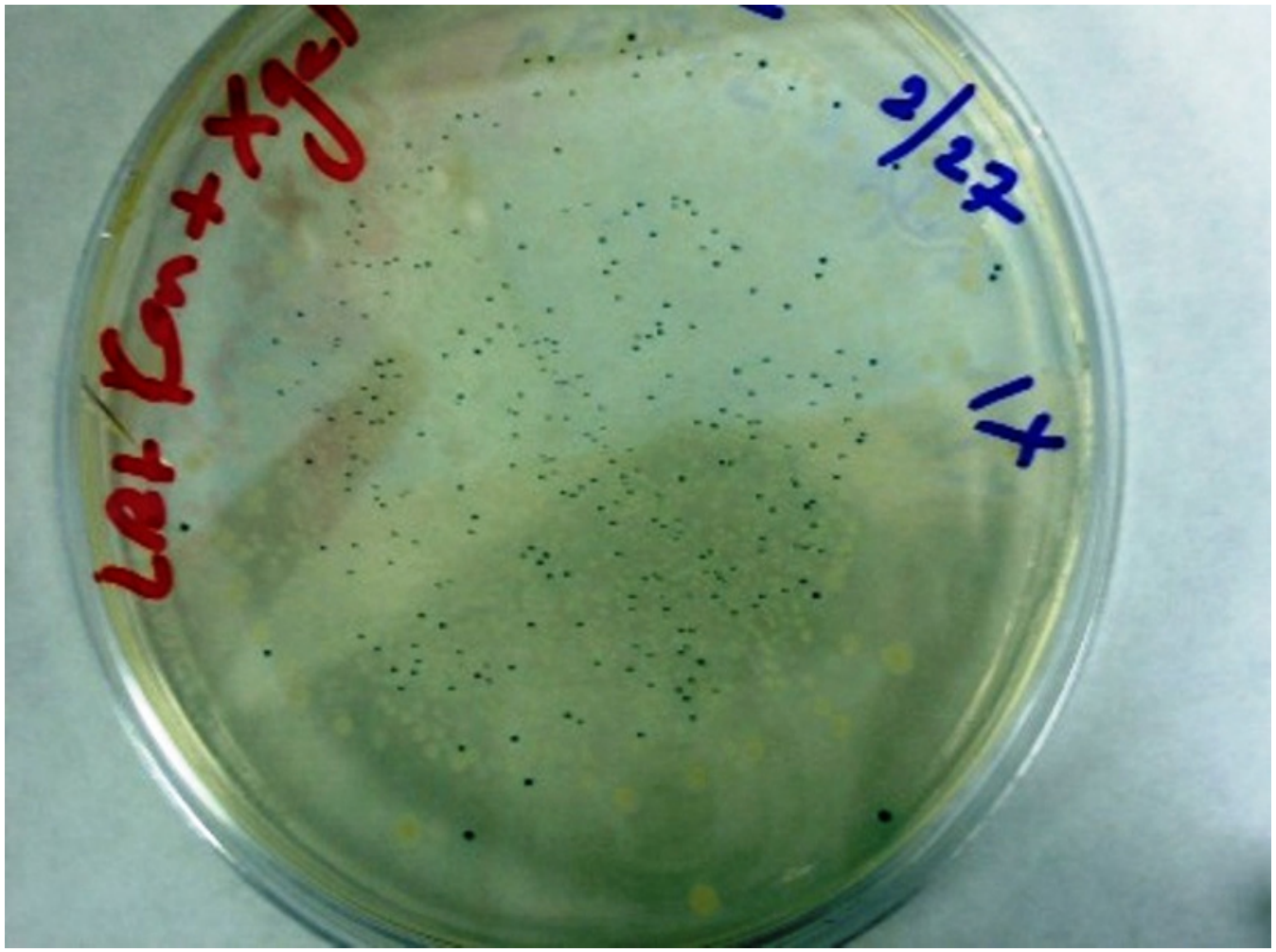

Figure A-3. Blue colonies of *E. coli* DH5α harboring plasmid pKD100

Step 5: Triparental Mating

Materials

LB broth
LB agar + kanamycin + X-gal
Colonies from Step 1(helper strain) and Step 4 (donor strain)
Paracoccus pantotrophus (recipient)

Procedure

- Three flasks, each containing 5mL of LB, were inoculated with, respectively, donor, helper and recipient strains from overnight cultures (5% inoculum) and were incubated in a shaker at 37˚C for two hours. Kanamycin to a final concentration of 25µg/mL was added in the growth medium of donor strain.

- Each culture is pelleted and resuspended in 2 mL LB to wash away the antibiotics.

- 150 µL donor strain and 150 µL helper strain was added to 450 µL of recipient strain and 5.0 mL of LB in a culture tube. The culture was incubated at 37°C for two hours in a shaker.

- The mixture was filtered through a 0.45 µm filter (Gelman Sciences, MI) and was placed cell side up on LB agar plate.

- The filter paper with the bacteria on it was resuspended in 5 mL LB and was put in the shaker at 37˚C for an hour.

- Several 10-fold serial dilutions were performed in LB. 100 µL of each dilution was plated on LB+kanamycin+Xgal agar and the plates were incubated at 37˚C.

- Ex-conjugants were kanamycin resistant, trimethoprim sensitive and the colonies were white on X-gal. Exconjugants were picked and streaked independently to get single colonies on the selective medium (LB agar+kanamycin+X-gal). The plates were incubated at 37˚C for a day.

Step 6: Confirmation of the Mutant

- PCR was carried out on genomic DNA of *P. pantotrophus* (negative control) and pKD100 (positive control) with same primers and same conditions used in Step 2.

- The PCR product was confirmed with Gel electrophoresis using λ/Hind III as the marker.

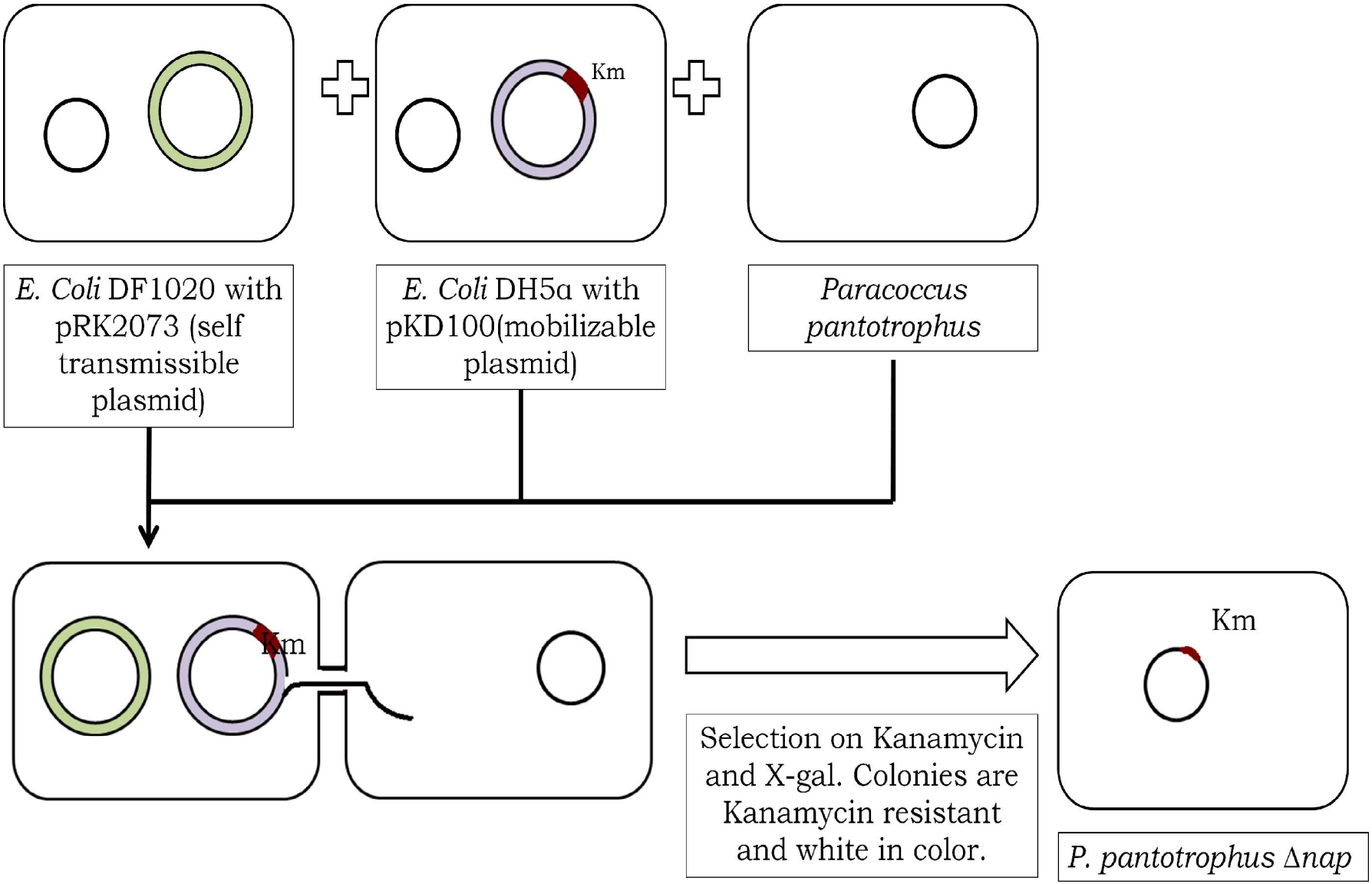

Figure A-4. Triparental mating

Figure A-5. Confirmation of the mutant (Lanes 1 and 8 – λ/*Hind* III marker, Lane 3 – Mutant, Lanes 4 and 5 – *P. pantotrophus* (negative control),Lane 6 – pKD100 (positive control)

APPENDIX B
DIFFERENTIAL EVOLUTION

Differential Evolution (DE) belongs to the class of evolution strategy optimizers which has a high probability of finding a global minimum of a multi-dimensional system. It is a stochastic, population based optimization algorithm introduced by Kenneth Price and Rainer Storn in 1996.

The objective function (cost function) that drives the optimization procedure was defined as Equation B-1, where g is a vector of $D\times1$ decision parameters (dimensions) and n is the number of data sets. The objective is to find a vector g in the given search space, for which the cost function is a minimum. The search space is defined by providing the lower and upper bounds for each of the $D\times1$ dimensions of g, i.e., $g^{min} \le g \le g^{max}$

$$\text{Min } F(g) = \sum_{n} \left(X_m - X_{cal}\right)^2 \tag{B-1}$$

The different steps in a DE algorithm are as follows

- Initialization
- Mutation
- Crossover/Recombination
- Selection

Initialization

The population (NP) to be sampled is usually taken as the 10 times the number of dimensions to be optimized. The population is randomly initialized. The result is an array of NP rows with D number of columns. In DE, the parameters are encoded as floating point numbers.

$$g_i^m = g^{min} + \text{rnd}() \times \left(g^{max} - g^{min}\right) \tag{B-2}$$

with i=1,2,3…NP and m=1…D and rnd () denotes a uniform random number generator.

Mutation

Three distinct random numbers (say a, b, c) are selected within the range, 1 to NP. The weighted difference of $\left(g_a^m - g_b^m\right)$ is used to perturb g_c^m to generate a noisy random vector, n_i^m:

$$n_i^m = g_c^m + F \times \left(g_a^m - g_b^m\right) \tag{B-3}$$

where i = 1. . . NP and m = 1. . . D. F is called the scaling factor and it is user-supplied within the range 0–1.2. This mutation ensures an efficient search of the solution space in each dimension.

Crossover/Recombination

Each primary population vector is recombined with a noisy random vector, n_i to generate a trial vector, t_i. Each trial vector parameter (t_i^m, where i=1. . . NP and m=1. . . D), is determined by a binomial experiment whose success or failure is determined by the user supplied crossover factor, CR ∈ [0,1].

$$\begin{aligned} t_i^m &= n_i^m, \text{ if rnd() > CR or m = D} \\ t_i^m &= g_i^m, \text{ otherwise} \end{aligned} \tag{B-4}$$

where i = 1, . . . , NP and m = 1, . . . , D

Therefore, trial vector, t_i, is the child of two parent vectors: noisy random vector, n_i and target vector, g_i. DE performs a non-uniform crossover, by virtue of which, the child vector can take more parameters from one parent than the other.

Selection

The trial vector competes with one of its parent vectors, target vector, and the fitter of the two (one with the lower cost value) proceeds to the next generation. The end of NP competitions will leave us with a new population. The procedure continues until the termination condition is reached, i.e. when the objective function attains a prescribed minimum or a specified number of generations are completed, whichever is earlier.

APPENDIX C
DIAUXIC GROWTH MODEL SOURCE CODE

```
# include <stdio.h>
# include <stdlib.h>
# include <math.h>

#define D 17
#define NP 170
#define gen_max 3000
#define CR 0.9
#define SF 0.8
#define IA 16807
#define IM 2147483647
#define AM (1.0/IM)
#define IQ 127773
#define IR 2836
#define NTAB 32
#define NDIV (1+ (IM-1)/NTAB)
#define EPS 1.2E-7
#define RNMX (1.0-EPS)

double obj1(double *g); /* sub-routine that calculates the cost of the objective function*/

double rnd(int *idum);   /* Uniform random number generator */

void result1(double *g); /* sub-routine that prints out the result */

main( )
{
      double score,var,r;
      int i,j,k,l,idum,count=0;
      double x2[NP][D],cost[NP],trial[NP],x1[NP][D],g[D];
      int x,y,z,p;

/* Parameters to be estimated are in the order:
Ks,ox,
Ks,an,
KOH,
KOi,
KNOi,
b,
bNO,
Yc,ox,
Yc,an,
νn,an,
K1,
```

K_2,
$a_{N,nar}$,
$V_{sni,}$
$\mu_{max,ox}$,
$\mu_{max,anox}$,
$e_{nar,initial}$
*/

/* Upper and lower bounds of the parameters to be estimated */

```
 double ll[ ]={0,0,0,0,0,0,0,0,0,0,0,0,0,0,0,0.5,0.01,1E-20};

double ul[ ]={.1,10,10,10,10,1,10,1,1,1,1E25,1E25,1E-3,1,1,0.1,1E-6};

idum=-22200;

for(p=0;p<NP;p++)
{
for(j=0;j<D;j++)
        {
                r=rnd(&idum);
                x1[p][j]=ll[j]+r*(ul[j]-ll[j]);
                g[j]=x1[p][j];
        }
        cost[p]=obj1(g);
 }
```

/* The above for loop randomly assigns values to the parameters between and lower and upper bounds and fills the population */

/* Differential evolution begins */

```
while(count<gen_max)
{

        for(p=0;p<NP;p++)
        {
                do x=(int)(rnd(&idum)*NP);while(x==p);
                do y=(int)(rnd(&idum)*NP);while(y==p||y==x);
                do z=(int)(rnd(&idum)*NP);while(z==p||z==x||z==y);

                for(k=0;k<D;k++)
                {
                        if(rnd(&idum)<CR||k==D-1)
                        {
                                trial[k]=x1[z][k]+(SF*(x1[x][k]-x1[y][k]));
                                if(trial[k]<ll[k])
```

```
                                        trial[k]=ll[k]+(ll[k]-trial[k])*(ul[k]-ll[k])/(ul[k]-
                                        trial[k]);
                                if(trial[k]>ul[k])
                                        trial[k]=ul[k]-(trial[k]-ul[k])*(ul[k]-ll[k])/(trial[k]-
                                        ll[k]);

                                g[k]=trial[k];
                        }
                        else
                        {
                                trial[k]=x1[p][k];
                                g[k]=trial[k];
                        }

                }

                score=obj1(g);


                if(score<=cost[p])
                {
                        for(j=0;j<D;j++)
                        {
                                x2[p][j]=trial[j];
                                cost[p]=score;
                        }
                }
                else
                {
                        for(j=0;j<D;j++)
                                x2[p][j]=x1[p][j];
                }
        }

        for(p=0;p<NP;p++)
        {
                for(j=0;j<D;j++)
                        x1[p][j]=x2[p][j];
        }
        count++;

}

var=cost[0];

for(i=0;i<NP;i++)
```

```
        {
                if(!(var<=cost[i]))
                {
                        l=i;
                        var=cost[i];
                }
        }

        for(j=0;j<D;j++)
                g[j]=x1[l][j];
        obj1(g);
        result1(g);
}
```

```
   /* Sub-routine to calculate the cost of the objective function using the parameters generated in
Differential evolution */

double obj1(double *g)
   {
      int k=0;

      double time[ ]={0.0,1.7,2.2,3.6,4.0,6.1,9.3,24.1,25.7,27.4};
      double cod[ ] = {18.360,42.840,81.260,209.440,226.440,278.120,302.260,
      351.220,406.640,461.040};
           int flag=1;
     double Ss=10000,Sn=400,en_nap,en_nar,So=8;
     double rate_ox,rate_an,rate_en_nar,rate_sni,fxb,fss,fsn,fen_nar,fsni,
    code[10],en_nar_max,sni_max;
     double Xe=0.0,Xb=18.36,sni=0;
     double i=0.0,deltai=0.01,anar,annar,Xa,Xan;
     en_nar=g[16];
     double mumax_ox=g[14],mumax_an=g[15];

      for(i=0.0;i<27.41;i+=0.01)
      {
            if((i >= 4.10)&&(flag == 1))
            {
             So=0.0;
             anar=en_nar;
             flag=0;
             }
             sni_max=g[13]/mumax_an-g[9];

             en_nar_max=g[12]/(g[5]+g[6])*((1+g[10]*sni_max)/(g[11]+g[10]*sni_max));
             if(Ss==0)
             {
                    rate_ox=0;
                    rate_an=0;
                    rate_sni=0;
                    rate_en_nar=0;
              }
              else
              {
                   rate_ox=mumax_ox*(Ss/(g[0]+Ss))*(So/(g[2]+So));

                   if(sni_max==0)
                         rate_an=0;
                   else
                         rate_an=mumax_an*(Ss/(g[1]+Ss))*(en_nar/en_nar_max)*(sni/sni_max);
                       rate_en_nar=g[12]*((1+g[10]*sni)/(g[11]+g[10]*sni))*(Ss/(Ss+g[1]));
```

```
            rate_sni=g[13]*(en_nar/en_nar_max)*(Sn/(Sn+g[4]))
                    *(g[3]/(g[3]+So))*(Ss/(Ss+g[1]));
    }

  fxb=(rate_ox+rate_an-g[5])*Xb;
  fss=(-(1/g[7])*rate_ox-(1/g[8])*rate_an)*Xb;
  fsn=-1*rate_sni*Xb;

  if(Xb==0)
  {
        fen_nar=0;
        fsni=0;
  }
  else
  {
        fen_nar=rate_en_nar-(g[5]+g[6]+fxb/Xb)*en_nar;
        fsni=rate_sni-g[9]*rate_an-(g[5]+fxb/Xb)*sni;
  }

   if(i==0.0)
   {
       code[k]=Xb;
        k=k+1;
   }

  Xb=Xb+fxb*deltai;
  Ss=Ss+fss*deltai;
  en_nar=en_nar+fen_nar*deltai;

  if (Ss<0)
     Ss=0;
  Sn=Sn+fsn*deltai;

  if (Sn<0)
     Sn=0;

  sni=sni+fsni*deltai;

  if(fabs(time[k]-(i+0.01))<0.000001)
  {
    code[k]=Xb;
     k=k+1;
   }

}
annar=en_nar;
```

```
        for(k=0;k<10;k++)
        {
                Xe=Xe+pow((cod[k]-code[k]),2);
        }
        Xa=pow((anar-0.42E-6),2);
        Xan=pow((annar-9.42E-6),2);
        Xe=Xe/pow(237.762,2)+(Xa+Xan)/pow(4.92E-6,2);
        return Xe;
}
```

/* Sub-routine result generates the predicted values after the parameters have been optimized by Differential evolution */

```
void result2(double *g)
  {
    int k=0;
    double time[ ]={0.00,1.7,2.2,3.6,4.0,6.1,9.3,24.1,25.7,27.4};
    double cod[ ] = {18.360,42.840,81.260,209.440,226.440,278.120,
     302.260,351.220,406.640,461.040};
    int flag=1;
    double Ss=10000,Sn=400,en_nap,en_nar,So=8;
    double rate_ox,rate_an,rate_en_nar,rate_sni,fxb,fss,fsn,fen_nar,fsni,
    code[10],en_nar_max,sni_max;
    double Xe=0.0,Xb=18.36,sni=0;
    double i=0.0,deltai=0.01;

    en_nar=g[16];
    double mumax_ox=g[14],mumax_an=g[15];

    FILE *fpt;
    fpt=fopen("resultskdnokanc.doc","w");

    for(i=0.0;i<27.41;i+=0.01)
    {

        fprintf(fpt,"\n%lf \t %e \t %lf \t %lf",i,en_nar,sni,Xb);

        if((i >= 4.10)&&(flag == 1))
        {
        So=0;
        flag=0;
        }
        sni_max=(g[13]/mumax_an-g[9]);

        en_nar_max=g[12]/(g[5]+g[6])*((1+g[10]*sni_max)/(g[11]+g[10]*sni_max));
         if(Ss==0)
        {
           rate_ox=0;
           rate_an=0;
           rate_sni=0;
           rate_en_nar=0;
        }
        else
        {
         rate_ox=mumax_ox*(Ss/(g[0]+Ss))*(So/(g[2]+So));
         if(sni_max==0)
```

```
            rate_an=0;
    else
            rate_an=mumax_an*(Ss/(g[1]+Ss))*(en_nar/en_nar_max)*(sni/sni_max);

    rate_en_nar=g[12]*((1+g[10]*sni)/(g[11]+g[10]*sni))*(Ss/(Ss+g[1]));

   rate_sni=g[13]*(en_nar/en_nar_max)*(Sn/(Sn+g[4]))*(g[3]/(g[3]+So))*(Ss/(Ss+g
   [1]));
}

fxb=(rate_ox+rate_an-g[5])*Xb;
fss=(-(1/g[7])*rate_ox-(1/g[8])*rate_an)*Xb;
fsn=-1*rate_sni*Xb;
if(Xb==0)
{
       fen_nar=0;
       fsni=0;
}
else
{
       fen_nar=rate_en_nar-(g[5]+g[6]+fxb/Xb)*en_nar;
       fsni=rate_sni-g[9]*rate_an-(g[5]+fxb/Xb)*sni;
}
if(i==0.0)
{
     code[k]=Xb;
     k=k+1;
}

Xb=Xb+fxb*deltai;
Ss=Ss+fss*deltai;
en_nar=en_nar+fen_nar*deltai;

if (Ss<0)
   Ss=0;
Sn=Sn+fsn*deltai;

if (Sn<0)
   Sn=0;

    sni=sni+fsni*deltai;

if(fabs(time[k]-(i+0.01))<0.000001)
{
 code[k]=Xb;
 k=k+1;
```

```
        }
    }
    for(k=0;k<10;k++)
    {
          Xe=Xe+pow(cod[k]-code[k],2);
    }
    fprintf(fpt,"\nOptimum cost=%e",Xe);
    fprintf(fpt,"\ne_nar=%e",en_nar);
    printf("\nOptimum cost=%e",Xe);
    getchar();
    for(k=0;k<D;k++)
    {
       fprintf(fpt,"\n%e",g[k]);
    }
    fclose(fpt);
}
```

```
/* Uniform random number generator */

double rnd(int *idum)
{
	int j;
	long k;
	static long iy=0;
	static long iv[NTAB];
	double temp;

	if(*idum <= 0 || !iy)
	{
		if(-(*idum) < 1)
			*idum=1;
		else
			*idum=-(*idum);
		for(j=NTAB+7;j>=0;j--)
		{
			k=(*idum)/IQ;
			*idum=IA*(*idum-k*IQ)-IR*k;
			if(*idum <0)
				*idum += IM;
			if(j<NTAB)
				iv[j] = *idum;
		}
		iy=iv[0];
	}
	k=(*idum)/IQ;
	*idum=IA*(*idum-k*IQ)-IR*k;
	if(*idum < 0)
		*idum += IM;
	j=iy/NDIV;
	iy=iv[j];
	iv[j] = *idum;
	if((temp=AM*iy) > RNMX)
		return RNMX;
	else
		return temp;
}
```

```
/* Model prediction for the wild-type*/

   # include <stdio.h>
   # include <stdlib.h>
   # include <math.h>

   #define D 7
   #define NP 70
   #define gen_max 1000
   #define CR 0.9
   #define SF 0.8
   #define IA 16807
   #define IM 2147483647
   #define AM (1.0/IM)
   #define IQ 127773
   #define IR 2836
   #define NTAB 32
   #define NDIV (1+(IM-1)/NTAB)
   #define EPS 1.2E-7
   #define RNMX (1.0-EPS)

   double obj1(double *g);
   double rnd(int *idum);
   void result1(double *g);

   main( )
   {
         double score,var,r;
         int i,j,k,l,idum,count=0;
         double x2[NP][D],cost[NP],trial[NP],x1[NP][D],g[D];
         int x,y,z,p;

         /* Parameters to be estimated are in the order:
         K_N,
         a_N,nap,
         η,
         e_nar,initial,
         e_nap,initial,
         μ_max,ox,
         μ_max,anox
         (rest of the parameters are same as that of the mutant*/


         double ll[ ]={0,0,0,1E-15,1E-15,0,0};
         double ul[ ]={5,1E-3,0.1,1E-8,1E-8,1,0.5};
         idum=-22200;
```

```
for(p=0;p<NP;p++)
{
        for(j=0;j<D;j++)
        {
                r=rnd(&idum);
                x1[p][j]=ll[j]+r*(ul[j]-ll[j]);
                g[j]=x1[p][j];
        }
        cost[p]=obj1(g);
}

while(count<gen_max)
{
        printf("\ncount = %d",count);
        for(p=0;p<NP;p++)
        {
                do x=(int)(rnd(&idum)*NP);while(x==p);
                do y=(int)(rnd(&idum)*NP);while(y==p||y==x);
                do z=(int)(rnd(&idum)*NP);while(z==p||z==x||z==y);

                for(k=0;k<D;k++)
                {
                        if(rnd(&idum)<CR||k==D-1)
                        {
                                trial[k]=x1[z][k]+(SF*(x1[x][k]-x1[y][k]));
                                if(trial[k]<ll[k])
                                        trial[k]=ll[k]+(ll[k]-trial[k])*(ul[k]-ll[k])/(ul[k]-
                                        trial[k]);
                                if(trial[k]>ul[k])
                                        trial[k]=ul[k]-(trial[k]-ul[k])*(ul[k]-ll[k])/(trial[k]-
                                        ll[k]);

                                g[k]=trial[k];

                        }
                        else
                        {
                                trial[k]=x1[p][k];
                                g[k]=trial[k];
                        }

                }


                score=obj1(g);
                if(score<=cost[p])
```

```
                {
                        for(j=0;j<D;j++)
                        {
                                x2[p][j]=trial[j];
                                cost[p]=score;
                        }
                }
                else
                {
                        for(j=0;j<D;j++)
                                x2[p][j]=x1[p][j];
                }
        }
        for(p=0;p<NP;p++)
        {
                for(j=0;j<D;j++)
                        x1[p][j]=x2[p][j];
        }
        count++;

    }
    var=cost[0];
    for(i=0;i<NP;i++)
    {
        if(!(var<=cost[i]))
        {
                l=i;
                var=cost[i];
        }
    }
    printf("\nOptimum result");
    printf("\ncost[%d] = %lf",l,cost[l]);
    getchar();
    for(j=0;j<D;j++)
    {
        g[j]=x1[l][j];
    }
    obj1(g);
    result1(g);
}
```

```
 /* Sub-routine to calculate the cost of the objective function using the parameters generated in
Differential evolution */

double obj1(double *g)
   {
     int k=0;
     double time[ ] = {0.0,1.3,1.8,2.4,3.4,3.8,4.4,5.1,5.9,6.9};
     double cod[ ] = {24.48,36.72,44.2,75.14,172.72,204.68,221.34,282.2,345.44,524.28};
     double h[ ] = {8.03E-02,1.60E+00,2.51E+00,5.98E+00,2.15E+00,1.74E-03,1.56E+00,
     9.19E-01,9.53E-01,2.26E-01,9.98E+24,9.63E+23,2.02E-05,6.53E-02};
     int flag=1;
     double Ss=1380,Sn=400,en_nap,en_nar,So=8;
     double rate_ox,rate_an,rate_en_nap,rate_en_nar,rate_sni,fxb,fss,fsn,fen_nar,
     fen_nap,fsni,code[10],en_nap_max,en_nar_max,sni_max;
     double Xe=0.0,Xb=24.48,sni=0,anar,anap,annap,annar,Xa,Xan;
     double i=0.0,deltai=0.01;
     en_nap=g[3];
     en_nar=g[4];
     double mumax_ox=g[5],mumax_an=g[6];

     for(i=0.0;i<6.9;i+=0.01)
         {
          if((i >= 3.8)&&(flag == 1))
        {
        So=0.0;
        anar=en_nar;
        anap=en_nap;
        flag=0;
        }
        sni_max=(h[13]/mumax_an-h[9]);
        en_nap_max=g[1]/(h[5]+h[6]);
        en_nar_max=h[12]/(h[5]+h[6])*((1+h[10]*sni_max)/(h[11]+h[10]*sni_max));

        if(Ss==0)
        {
               rate_ox=0;
               rate_an=0;
               rate_sni=0;
               rate_en_nap=0;
               rate_en_nar=0;
         }
         else
         {
         rate_ox=mumax_ox*(Ss/(h[0]+Ss))*(So/(h[2]+So));
         if(sni_max==0)
                    rate_an=0;
```

```
 else
            rate_an=mumax_an*(Ss/(h[1]+Ss))*((1-g[2])*(en_nar/en_nar_max)*
              (sni/sni_max)+g[2]*(en_nap/en_nap_max)*Sn/(g[0]+Sn));

rate_en_nap=g[1]*(So/(So+h[2]))*(Sn/(Sn+g[0]));
rate_en_nar=h[12]*((1+h[10]*sni)/(h[11]+h[10]*sni))*(Ss/(Ss+h[1]));
rate_sni=h[13]*(en_nar/en_nar_max)*(Sn/(Sn+h[4]))*(h[3]/(h[3]+So))*(Ss/(Ss+h[1]));
}

fxb=(rate_ox+rate_an-h[5])*Xb;
fss=(-(1/h[7])*rate_ox-(1/h[8])*rate_an)*Xb;
fsn=-1*rate_sni*Xb;
if(Xb==0)
{
        fen_nar=0;
        fen_nap=0;
        fsni=0;
}
else
{
        fen_nar=rate_en_nar-(h[5]+h[6]+fxb/Xb)*en_nar;
        fen_nap=rate_en_nap-(h[5]+h[6]+fxb/Xb)*en_nap;
        fsni=rate_sni-h[9]*rate_an-(h[5]+fxb/Xb)*sni;
}

if(i==0.0)
    {
   code[k]=Xb;
k=k+1;
}

Xb=Xb+fxb*deltai;
Ss=Ss+fss*deltai;
en_nap=en_nap+fen_nap*deltai;
en_nar=en_nar+fen_nar*deltai;

if (Ss<0)
  Ss=0;
Sn=Sn+fsn*deltai;

if (Sn<0)
  Sn=0;
  sni=sni+fsni*deltai;

if(fabs(time[k]-(i+0.01))<0.000001)
{
```

```
        code[k]=Xb;
        k=k+1;
      }
    }
    annar=en_nar;
    annap=en_nap;
    for(k=0;k<10;k++)
    {
                Xe=Xe+pow((cod[k]-code[k]),2);
    }
    Xa=pow((anar-0.31E-6),2)+pow((annar-16.3E-6),2);
    Xan=pow((annap-1.33E-6),2)+pow((anap-2E-6),2);
    Xe=Xe/pow(193.12,2)+Xa/pow(8.31E-6,2)+Xan/pow(1.67E-6,2);
    return Xe;
}
```

```
/* Sub-routine result generates the predicted values after the parameters have been optimized by
Differential evolution */

   void result1(double *g)
   {
     int k=0;
     double time[ ]={0.0,1.3,1.8,2.4,3.4,3.8,4.4,5.1,5.9,6.9};
     double cod[ ] = {24.48,36.72,44.2,75.14,172.72,204.68,221.34,282.2,345.44,524.28};
     int flag=1;
     double Ss=1380,Sn=400,en_nap,en_nar,So=8;
     double rate_ox,rate_an,rate_en_nap,rate_en_nar,rate_sni,fxb,fss,fsn,
     fen_nar,fen_nap,fsni,code[10],en_nap_max,en_nar_max,sni_max;
     double Xe=0.0,Xb=24.48,sni=0;
     double i=0.0,deltai=0.01;
    double h[ ] = {8.03E-02,1.60E+00,2.51E+00,5.98E+00,2.15E+00,1.74E-03,1.56E+00,
    9.19E-01,9.53E-01,2.26E-01,9.98E+24,9.63E+23,2.02E-05,6.53E-02};
     en_nap=g[3];
     en_nar=g[4];
     double mumax_ox=g[5],mumax_an=g[6];

     FILE *fpt;
     fpt=fopen("resultsppfopt.doc","w");

     for(i=0.0;i<6.9;i+=0.01)
     {
          fprintf(fpt,"\n%lf \t %e \t %e \t %lf \t %lf",i,en_nar,en_nap,sni,Xb);

          if((i >= 3.8)&&(flag == 1))
        {
        So=0.0;
        flag=0;
        }
        sni_max=(h[13]/mumax_an-h[9]);
        en_nap_max=g[1]/(h[5]+h[6]);
        en_nar_max=h[12]/(h[5]+h[6])*((1+h[10]*sni_max)/(h[11]+h[10]*sni_max));

        if(Ss==0)
        {
                rate_ox=0;
                rate_an=0;
                rate_sni=0;
                rate_en_nap=0;
                rate_en_nar=0;
         }
         else
         {
```

```
 rate_ox=mumax_ox*(Ss/(h[0]+Ss))*(So/(h[2]+So));
 if(sni_max==0)
            rate_an=0;
 else
            rate_an=mumax_an*(Ss/(h[1]+Ss))*((1-g[2])*(en_nar/en_nar_max)*
              (sni/sni_max)+g[2]*(en_nap/en_nap_max)*Sn/(g[0]+Sn));

rate_en_nap=g[1]*(So/(So+h[2]))*(Sn/(Sn+g[0]));
rate_en_nar=h[12]*((1+h[10]*sni)/(h[11]+h[10]*sni))*(Ss/(Ss+h[1]));
rate_sni=h[13]*(en_nar/en_nar_max)*(Sn/(Sn+h[4]))*(h[3]/(h[3]+So))*(Ss/(Ss+h[1]));
}

fxb=(rate_ox+rate_an-h[5])*Xb;
fss=(-(1/h[7])*rate_ox-(1/h[8])*rate_an)*Xb;
fsn=-1*rate_sni*Xb;
if(Xb==0)
{
        fen_nar=0;
        fen_nap=0;
        fsni=0;
}
else
{
        fen_nar=rate_en_nar-(h[5]+h[6]+fxb/Xb)*en_nar;
        fen_nap=rate_en_nap-(h[5]+h[6]+fxb/Xb)*en_nap;
        fsni=rate_sni-h[9]*rate_an-(h[5]+fxb/Xb)*sni;
}

if(i==0.0)
    {
   code[k]=Xb;
k=k+1;
}

Xb=Xb+fxb*deltai;
Ss=Ss+fss*deltai;
en_nap=en_nap+fen_nap*deltai;
en_nar=en_nar+fen_nar*deltai;

if (Ss<0)
  Ss=0;
Sn=Sn+fsn*deltai;

if (Sn<0)
  Sn=0;
  sni=sni+fsni*deltai;
```

```
    if(fabs(time[k]-(i+0.01))<0.000001)
    {
      code[k]=Xb;
      k=k+1;
    }
  }
  for(k=0;k<10;k++)
  {
                Xe=Xe+pow(cod[k]-code[k],2);
  }
  fprintf(fpt,"\nOptimum cost=%e",Xe);
  fprintf(fpt,"\ne_nar=%e\ten_nap=%e",en_nar,en_nap);
  printf("\nOptimum cost=%e",Xe);
  getchar();
  for(k=0;k<D;k++)
  {
      fprintf(fpt,"\n%e",g[k]);
  }
    fclose(fpt);
}
```

LIST OF REFERENCES

Bedzyk L, Wang T, Ye RW. 1999. The periplasmic nitrate reductase in *Pseudomonas* sp. strain G-179 catalyzes the first step of denitrification. J Bacteriol 181: 2802-2806.

Bell LC, Richardson DJ, Ferguson SJ. 1990. Periplasmic and membrane-bound respiratory nitrate reductases in *Thiosphaera pantotropha*: the periplasmic enzyme catalyzes the first step in aerobic denitrification. FEBS Letters 265: 85-87.

Berks BC, Ferguson SJ, Moir JWB, Richardson DJ. 1995. Enzymes and associated electron transport systems that catalyse the respiratory reduction of nitrogen oxides and oxyanions. Biochimica et BiophysicaActa 1232: 97-173.

Berks BC, Richardson DJ, Reilly A, Willis AC and Ferguson SJ. 1995. The *napEDABC* cluster encoding the periplasmic nitrate reductase system of *Thiosphaera pantotropha.* Biochem J 309: 983-992.

Berks BC, Richardson DJ, Robinson C, Reilly A, Aplin RT, Ferguson SJ. 1994. Purification nd characterization of the periplasmic nitrate reductase from *Thiosphaera pantotropha.* Eur J Biochem 220: 117-124.

Cancer Genetics, Inc. 2004. Fluorescent in situ hybridization (FISH) protocol. Retrieved May 16, 2007, from Cancer Genetics, Inc: www.cancergenetics.com

Casasús IA. 2001. Effect of exposure to oxygen on the diauxic lag. Masters Thesis. University of Florida, Gainesville, Florida.

Casasús IA, Lee D, Hamilton R, Svoronos SA, Koopman B. 2007. Effect of carbon substrate on electron acceptor diauxic lag and anoxic maximum specific growth rate in species with and without periplasmic enzyme. J Environ Sci Health A Tox Hazard Subst Environ Eng 42: 103-108.

Datsenko KA, Wanner BL. 2000. One-step inactivation of chromosomal genes in *Escherichia coli* K-12 using PCR products. PNAS 97: 6640-6645.

Durvasula K, Jantama K, Fischer K,Vega A, Koopman B, Svoronos SA. Effect of periplasmic nitrate reductase (Nap) on diauxic lag of *Paracoccus pantotrophus* (submitted to Biotechnology Progress, AICHE).

Ellington MJK, Bhakoo KK, Sawers G, Richardson DJ, Ferguson SJ. 2002. Hierarchy in Carbon Source Selection in *Paracoccus pantotrophus* between Reduction State of the Carbon Substrate and Aerobic Expression of the *nap* Operon. Journal of Bacteriology 184: 4767-4774.

Goldberg JB, Ohman DE. 1984. Cloning and expression in *P. aeruginosa* of a gene involved in the production of alginate. J Bacteriol 158:1115-1121.

Gouw M, Bozic R, Koopman B, Svoronos SA. 2001. Effect of nitrate exposure history on the oxygen/nitrate diauxic growth of *Pseudomonas denitrificans*. Water Res 35: 2794-2798.

Grady L, Daigger GT, Lim HC. 1999. Biological Wastewater Treatment. New York: Marcel Dekker, Inc.

Grunstein M, Hogness DS. 1975. Colony hybridization: a method for the isolation of cloned DNAs that contain a specific gene. PNAS 72: 3961-3965.

Hamilton R, Casasús A, Rasche M, Narang A, Svoronos SA, Koopman B. 2005. A structured model for denitrifier diauxic growth. Biotechnol Bioeng 90: 501-508.

Henegariu O, Heerema N, Wright LL, Bray-Ward P, Ward D C, Vance GH. 2000. Improvements in Cytogenetic Slide Preparation: Controlled Chromosome Spreading, Chemical Aging and Gradual Denaturing. Cytometry 43:101-109.

Henze M, Gujer W, Mino T, Loosdrecht MV. 2000. Activated sludge models ASM1, ASM2, ASM2d and ASM3. Number 9 in Scientific and Technical Report, International Water Association, London.

Jones RW, Gray TA, Garland PB.1976. A study of the permeability of the cytoplasmic membrane of Escherichia coli to reduced and oxidized benzyl viologen and methyl viologen cations: complications in the use of viologens as redox mediators for membrane-bound enzymes. Biochem Soc Trans 4: 671-673.

Kodama T, Shimada K, Mori T. 1969. Studies on anaerobic biphasic growth of a denitrifying bacterium, *Pseudomonas stutzeri*. Plant and Cell Physiology 10: 855-865.

Kompala DS, Ramkrishna D, Jansen NB, Tsao GT. 1986. Investigation of bacterial growth on mixed substrates: Experimental evaluation of cybernetic models. Biotechnology and Bioengineering 28: 1044-1055.

Lee DU, Woo SH, Svoronos SA, Koopman B. 2008. Determination of diauxic lag in continuous culture. Biotechnol Bioeng. doi: 10.1002/bit. 21925.

Lighton K, Fiandaca MJ. 2005. Fluorescence measurement of hybridization between quencher (DABCYL) labelled PNA probes and a fluoresceine labelled DNA using the Fluorescence BioMelt™ Package. VarianInc.

Lisbon K, McKean M, Shekar S, Svoronos SA, Koopman B. 2002. Effect of DO on oxic/anoxic diauxic lag of *Pseudomonas denitrificans*. Journal of Environmental Engineering 128: 391-394.

Liu PH, Svoronos SA, Koopman B. 1998b. Experimental and modeling study of diauxic lag of *Pseudomonas denitrificans* switching from oxic and anoxic conditions. Biotechnol Bioeng 60: 649-655.

Liu PH, Zhan G, Svoronos, SA, Koopman B.1996. Cybernetic Approach to Modeling Denitrification in Activated Sludge. Presented at 1996 AIChE National Meeting, Chicago.

Liu PH, Zhan G, Svoronos SA, Koopman B. 1998a. Diauxic lag from changing electron acceptors in activated sludge treatment. Water Res 32: 3452-3460.

Mendenhall W and Sincich T. 2007. Statistics for engineering and sciences, 5th Ed. Pearson Prentice Hall Upper saddle river New Jersey.

Monod J. 1942. The growth of bacterial cultures. Annu Rev Micobiol 3: 371-394.

Moreno-Vivián C, Cabello P, Martínez-Luque M, Blasco R, Castillo F. 1999. MiniReview-Prokaryotic nitrate reduction: Molecular properties and functional distinction among bacterial nitrate reductases. J Bacteriol 181: 6573-6584.

Nikaido H. 2003. Molecular Basis of Bacterial Outer Membrane Permeability Revisited. Microbiol Mol Biol Rev 67: 593-656.

Oh J, Silverstein J. 1999b. Effect of air on-off cycles on activated-sludge denitrification. Water Environment Research 71: 1276-1282.

Ramalho, R S. 1983. Introduction to Wastewater Treatment Processes. San Diego, California: Academic Press.

Richardson DJ, Ferguson SJ. 1992. The influence of carbon substrate on the activity of the periplasmic nitrate reductase in aerobically grown *Thiosphaera pantotropha*. Arch Microbiol 157: 535-537.

Rusmana I, Nedwell BD. 2004. Use of chlorate as a selective inhibitor to distinguish membrane-bound nitrate reductase (Nar) and periplasmic nitrate reductase (Nap) of dissimilative nitrate reducing bacteria in sediment. FEMS Microbiology Ecology 48: 379-386.

Sambrook J, Fritsch EF, Maniatis T. 1989. Molecular Cloning: a Laboratory Manual. 2nd Ed. New York: Cold Spring Harbor, Cold Spring Harbor Laboratory.

Sear HJ, Sawers G, Berks BC, Ferguson SJ, Richardson DJ. 2000. Control of periplasmic nitrate reductase gene expression (*napEDABC*) from *Paracoccus pantotrophus* in response to oxygen and carbon substrates. Microbiol 146: 2977-2985.

Shoemaker J, Reeves GT, Gupta S, Pilyugin SS, Egli T, Narang A. 2003. The dynamics of single-substrate continuous cultures: the role of transport enzymes. J Theor Biol 222: 307-322.

Siddiqui RA, Warnecke-Eberz U, Hengsberger A, Schneider B, Kostka S, Friedrich B. 1993. Structure and function of a periplasmic nitrate reductase in *Alcaligenes eutrophus* H16. J Bacteriol 175: 5867-5876.

Storn R, Price K. 1997. Differential Evolution – A simple evolution strategy for fast optimization. Dr. Dobb's Journal 22:18–24.

Tiedje JM. 1988. Ecology of denitrification and dissimilatory nitrate reduction to ammonium. In Biology of Anaerobic Microorganisms. New York : Wiley and Sons.

Van Spanning RJM, Wansell CW, Reijnders WN, Harms N, Ras J, Oltmann LF, Stouthamer AH. 1991. A method for introduction of unmarked mutations in the genome of *Paracoccus pantotrophus:* Construction of strains with multiple mutations in the genes encoding periplasmic cytochromes c550, c551i, and c553i. J Bacteriol 173: 6962-6970.

Vishniac W, Santer M. 1957. The thiobacilli. Bacteriol Rev. 21(3): 195-213.

Waki T, Murayama K, Kawato Y, Ichikawa K. 1980. Transient characteristics of *Paracoccus denitrificans* with changes between aerobic and anaerobic conditions. Journal of Fermentation Technology 58: 243-249.

Warnecke-Eberz U, Friedrich B. 1993. Three nitrate reductase activities in *Alcaligenes eutrophus.* Archives of Microbiology 159: 405-409.

Wilderer AP, Bungartz Joachim-Hans, Lemmer H, Wagner M, Keller J, Wuertz S. 2002. Modern Scientific methods and their potential in wasterwater science and technology. Water Research 36: 370-393.

Wood JN, Alizadeh T, Richardson DJ, Ferguson SJ, Moir JWB. 2002. Two domains of a dual-function NarK protein are required for nitrate uptake, the first step of denitrification of *Paracoccus pantotrophus*. Molecular Microbiology 44: 157-170.

Yagil G, Yagil E. 1971. On the relation between effector concentration and the rate of induced enzyme synthesis. Biophys J 11: 11-27.

BIOGRAPHICAL SKETCH

Kiranmai Durvasula (Kiran) was born in 1982 in Visakhapatnam, India. She received her Bachelor of Engineering (hons.) degree in chemical engineering in 2003 from Birla Institute of Technology, Pilani (BITS, Pilani), India. In 2004, she began her doctoral study in the Department of Chemical Engineering at University of Florida, Gainesville and received her doctorate in 2008. She was a recipient of Alumni fellowship during her graduate studies. Her research interests include biological nitrate removal, modeling biological systems and genetic engineering.